Supplementary Materials for

Stable Monovalent Aluminum(I) in Reduced Phosphomolybdate Cluster as Active Acid Catalyst

Ya-Qi Zhang,[a,⑤] Lai-Yun Zhou,[a,⑤] Yuan-Yuan Ma,[a,*] Kamran Dastafkan,[b] Chuan Zhao,[b] Lan-Zhi Wang,[a,*] Zhan-Gang Han[a,*]

[a] Y-Q Zhang, L-Y Zhou, Y-Y Ma, L-Z Wang, Z-G Han

Hebei Key Laboratory of Organic Functional Molecules, National Demonstration Center for Experimental Chemistry Education, College of Chemistry and Material Science, Hebei Normal University, Shijiazhuang, Hebei 050024, People's Republic of China.

[b] K Dastafkan, C Zhao

School of Chemistry, The university of New South Wales, Sydney, NSW 2052, Australia.

⑤ Y. Q. Zhang and L. Y. Zhou contributed equally to this work.

Correspondence to: mayy334@hebtu.edu.cn; wanglanzhi@126.com; hanzg116@126.com; hanzg116@hebtu.edu.cn

Table of Contents

Materials and Methods

Materials and Characterizations

All chemical reagents are obtained commercially and used directly without any treatment. FTIR spectra (KBr pellet) were recorded with a FTIR-8900 IR spectrometer in the range of 400–4000 cm^{-1}. TG analyses were performed on a Perkin-Elmer Pyris Diamond TG/DTA instrument in flowing N_2 with a heating rate of 10 °C min^{-1}. XRD patterns were conducted using a Bruker AXS D8 Advance diffractometer. Energy-dispersive spectroscopy (EDS) were conducted on a cold field-emission scanning electron microscope (S-4800). The **$Al_6\{P_4Mo_6\}_6$** and **$Al\{P_4Mo_6\}_2$** catalyst was investigated using a Leeman Prodigy Spec inductively coupled plasma atomic emission spectrometer (ICP-AES).

Synthesis

A mixture of $Na_2MoO_4{\cdot}2H_2O$ (0.12 g, 0.50 mmol), $Al(NO_3)_3{\cdot}9H_2O$ (0.08 g, 0.21 mmol), bpe (0.03 g, 0.16 mmol), bpp (0.03 g, 0.15 mmol), H_3PO_4 (0.50 mL, 7.50 mmol) and H_2O (8 mL, 0.44 mol) was stirred for half an hour at room temperature, and the pH was adjusted to 1.5 with 4M NaOH. The mixture was transferred to a 20 mL Teflon-lined stainless-steel container and heated to 160 °C for 5 days. It was lowered to room temperature at a rate of 8 °C h^{-1}, and after washed and dried, the pure red strip crystals of **$Al_6\{P_4Mo_6\}_6$** were isolated (yield 68% based on Mo). Elemental analysis calculated for $C_{132}H_{200}Al_6Mo_{36}N_{22}O_{201}P_{24}$ (%): C, 16.39; H, 2.08; N, 3.19. Found (%): C, 16.27; H, 2.10; N, 3.15. The preparation of hybrid **$Al\{P_4Mo_6\}_2$** was similar to the method of **$Al_6\{P_4Mo_6\}_6$**, except that the pH value was adjusted to 0.5 with 8M H_3PO_4. Red block crystals were obtained (yield 55% based on Mo).

Single-crystal X-ray diffraction

Crystal data were collected on a SMART APEX II CCD Area Detector diffractometer using Mo Kα radiation (λ = 0.71073 Å) at 296(2) K. Then the collected data were analyzed using the SHELEXL program, the results were corrected using the full matrix least squares method, and anisotropic correction was performed for all non-hydrogen atoms. The hydrogen atoms connected to the carbons were added to the geometric ideal position, the hydrogen atoms of water molecule were not specified, but were directly added to the final molecular formula. The crystal data information of **$Al_6\{P_4Mo_6\}_6$** and **$Al\{P_4Mo_6\}_2$** is shown in Table S1 (CCDC: 1970141 for **$Al_6\{P_4Mo_6\}_6$**; 1970140 for **$Al\{P_4Mo_6\}_2$**).

Determination of acidity.

The acidity (mmol g^{-1}) of the **$Al_6\{P_4Mo_6\}_6$** and **$Al\{P_4Mo_6\}_2$** was determined by the neutralization titration method. Typically, catalyst (0.1 g) was added to an aqueous solution of NaCl (2.0 mol L^{-1}, 20.0 mL). The mixture was stirred for 24 h at room temperature. After filtered, the clear solution was titrated with aqueous NaOH (6.0 mmol L^{-1}) with phenolphthalein as the indicator.

Catalysis.

General catalytic procedure of four-component domino reaction for the solvent-free one-pot synthesis of 1,5-benzodiazepines was described as follows: a mixture of aromatic ketone (1.00 mmol), *N,N*-dimethylformamide dimethyl acetal (1.00 mmol) and catalysts (10.00 mg) were heated at 60 °C with constant stirring for 3.0 h. After the completion of reaction monitored by

TLC, 1,2-phenylenediamine (1.00 mmol) was added to the same reaction flask, respectively. Then, the resulting reaction mixture was further subjected to heating at 60 ^{o}C for the time indicated in Table 1. After completion of reaction monitored by TLC, ketone derivative (1.00 mmol) was added to the same reaction flask and stirred at 30 ^{o}C for 20 min. After that, the crude reaction mass was dissolved in ethyl acetate (10.00 mL). To recover the catalysts, the ethyl acetate portion was centrifuged and filtered. From the residue, POM catalyst was isolated and the filtrate (ethyl acetate layer) was then washed with water (3 × 10.00 mL) and brine (1 × 10.00 mL), and dried over anhydrous Na_2SO_4. The reaction mixture was then concentrated under vacuum and purified by column chromatography using petroleum ether–ethyl acetate as the eluent.

Supplementary Figures

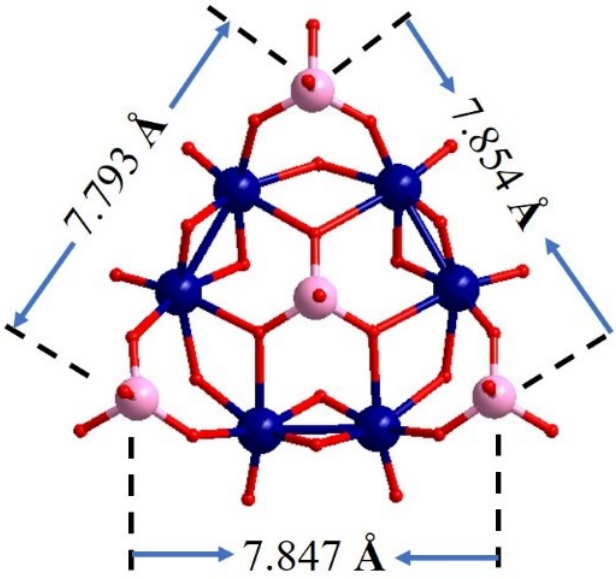

Figure S1. The side sizes of $\{P_4Mo_6\}$ subunit.

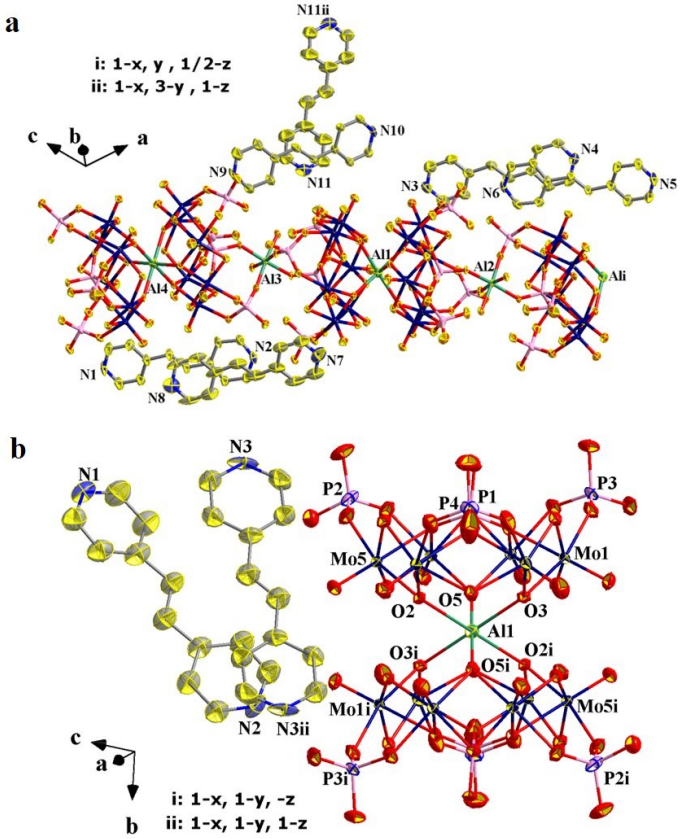

Figure S2. ORTEP views of the asymmetric unit in $\mathbf{Al_6\{P_4Mo_6\}_6}$ (a) and $\mathbf{Al\{P_4Mo_6\}_2}$ (b).

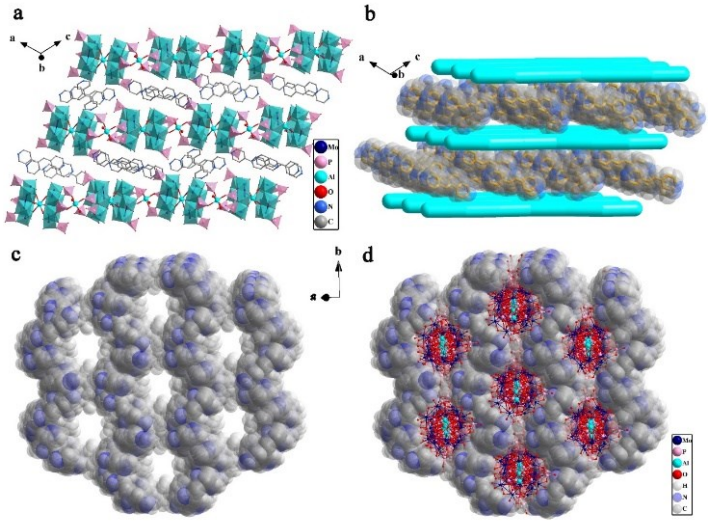

Figure S3. (a) Packing mode of 1D inorganic anions and organic cations in **$Al_6\{P_4Mo_6\}_6$**. (b) Space-filling views showing the stacking modes of inorganic and organic moieties in **$Al_6\{P_4Mo_6\}_6$**. (c-d) Space-filling view showing the honeycomb-like supramolecular organic moiety to accommodate 1D inorganic chains *via* intermolecular forces.

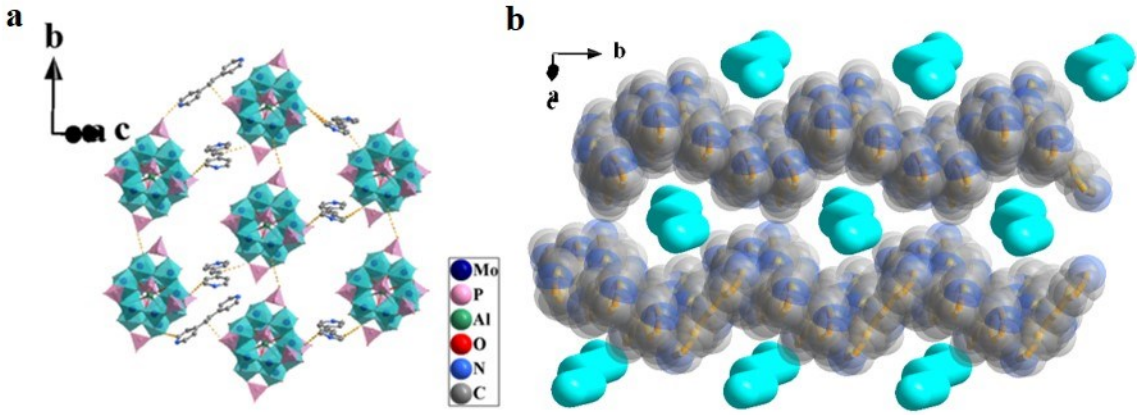

Figure S4. (a) 2D inorganic-organic network in **$Al_6\{P_4Mo_6\}_6$**. (b) Schematic views showing the packing mode of the inorganic and space-filling view showing the 3D stacked structure of bpe in **$Al_6\{P_4Mo_6\}_6$**.

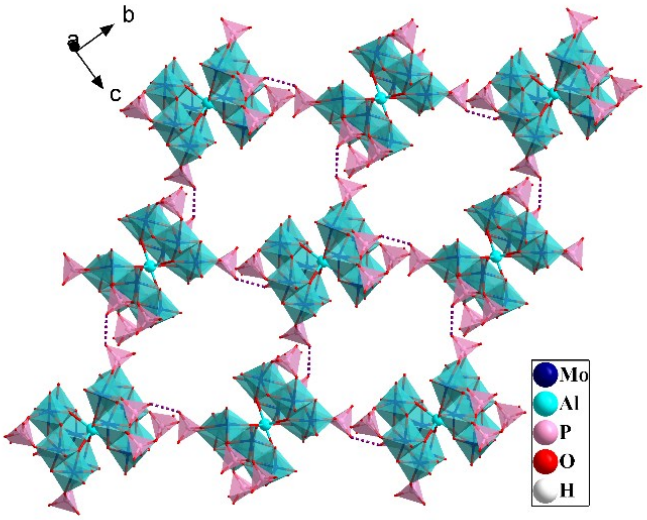

Figure S5. 2D inorganic network in **Al{P_4Mo_6}$_2$**.

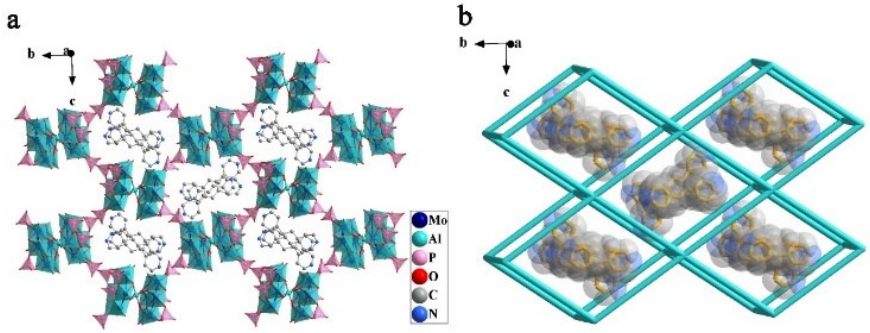

Figure S6. (a) 2D network structure in **Al{P_4Mo_6}$_2$**. (b) Schematic view showing the packing mode of the simplified inorganic moiety and space-filling bpe cations in **Al{P_4Mo_6}$_2$**.

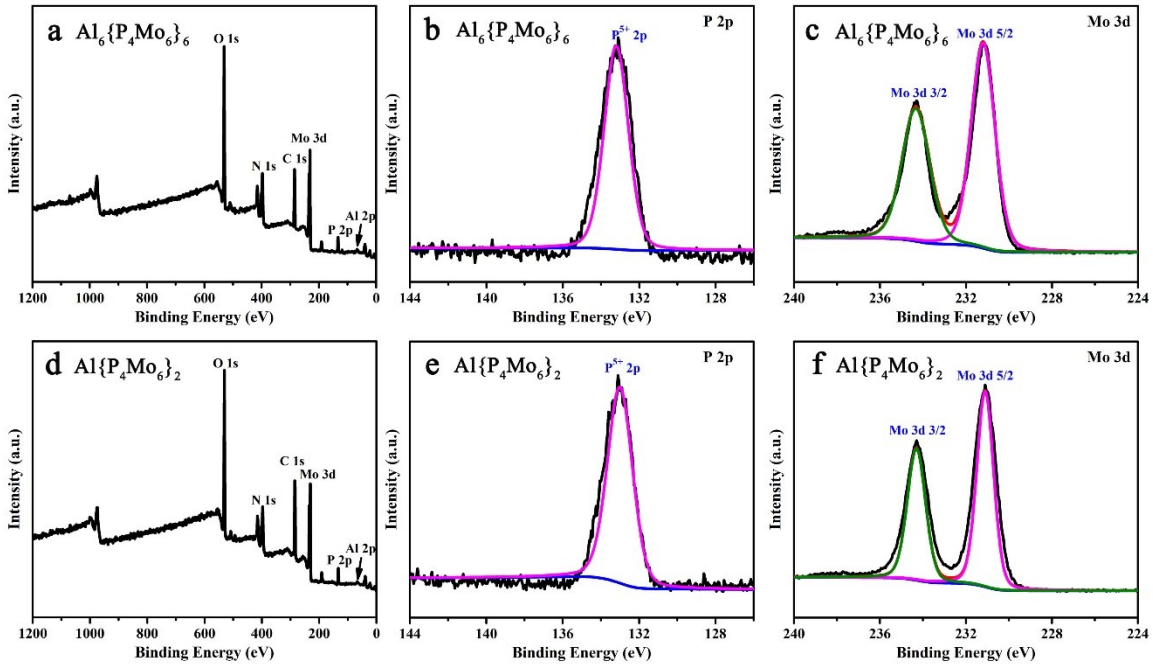

Figure S7. XPS spectra (a-c) of **$Al_6\{P_4Mo_6\}_6$**. (d-f) of **$Al\{P_4Mo_6\}_2$**.

	Elements	Weight %	Atom %
$Al_6\{P_4Mo_6\}_6$	C K	34.50	57.40
	O K	23.75	29.66
	P K	7.83	5.05
	Al K	1.54	1.14
	Mo L	32.37	6.74
	Sum	100.00	
$Al\{P_4Mo_6\}_2$	C K	32.52	52.15
	N K	7.88	10.84
	O K	22.27	26.81
	P K	6.06	3.77
	Al K	0.30	0.22
	Mo L	30.97	6.22
	Sum	100.00	

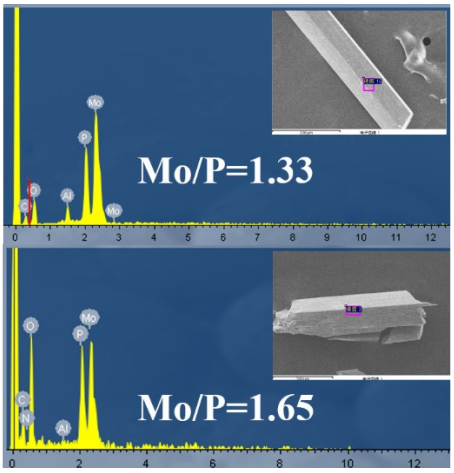

Figure S8. EDS spectra of crystals **$Al_6\{P_4Mo_6\}_6$** and **$Al\{P_4Mo_6\}_2$**.

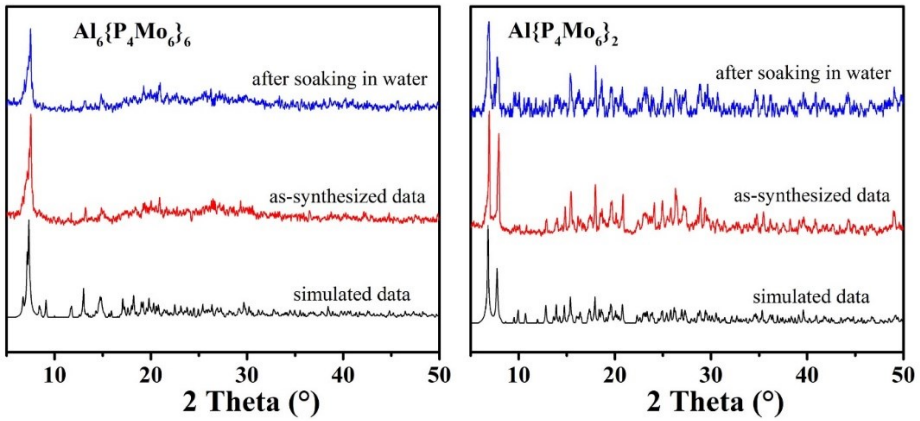

Figure S9. XRD patterns of **$Al_6\{P_4Mo_6\}_6$** and **$Al\{P_4Mo_6\}_2$** after immersing in water for 24 hours.

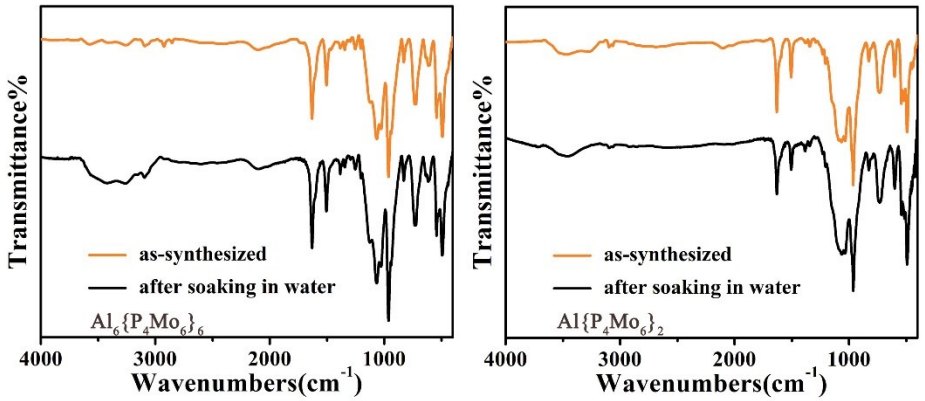

Figure S10. IR spectra of **$Al_6\{P_4Mo_6\}_6$** and **$Al\{P_4Mo_6\}_2$** after immersing in water for 24 hours.

The IR spectra of **$Al_6\{P_4Mo_6\}_6$** and **$Al\{P_4Mo_6\}_2$** were recorded between 4000 and 400 cm^{-1}, as shown in Figure S10. All supramolecular assemblies **$Al_6\{P_4Mo_6\}_6$** and **$Al\{P_4Mo_6\}_2$** exhibit the characteristic peaks of the $\{P_4Mo_6\}$ polyoxoanion: the characteristic bands in the range of 540-730 cm^{-1} are attributed to ν(Mo-O-Mo) vibrations; strong peaks at 950- 995 cm^{-1} are due to ν(Mo=O) vibrations; the ν(P=O) vibration ranges from 1020- 1130 cm^{-1}. The feature peaks in 1500- 1630 cm^{-1} ranges are assigned to the stretching vibrations of C=C and C=N bonds of bpe ligands. The broad bands at 2900- 3440 cm^{-1} are associated with C-H, N-H and O-H bending and stretching vibrations, further proving that there are extensive hydrogen bonding interactions among the supramolecular frameworks of **$Al_6\{P_4Mo_6\}_6$** and **$Al\{P_4Mo_6\}_2$**.

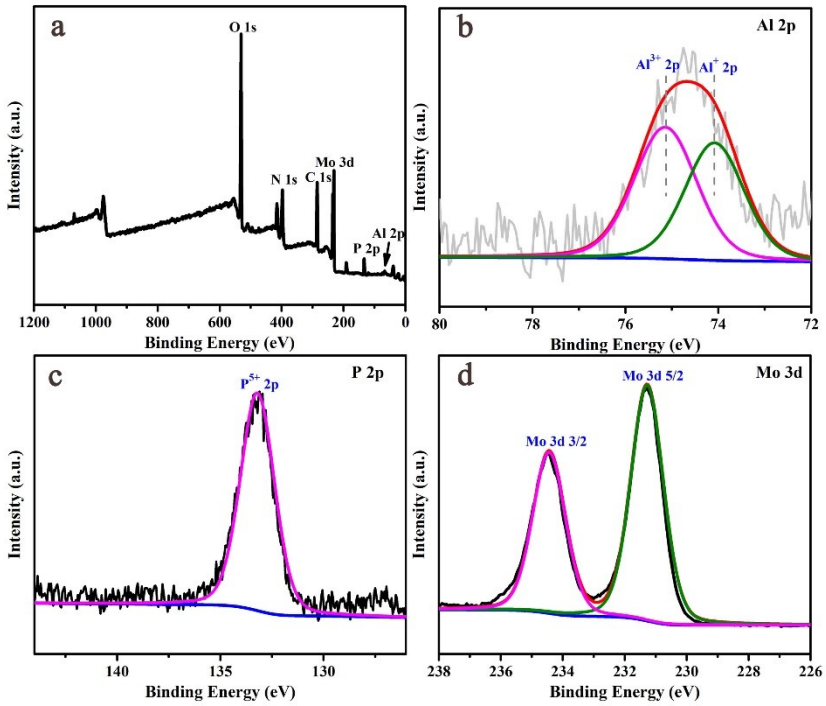

Figure S11. XPS spectra of **$Al_6\{P_4Mo_6\}_6$** after immersing in water for 24 hours.

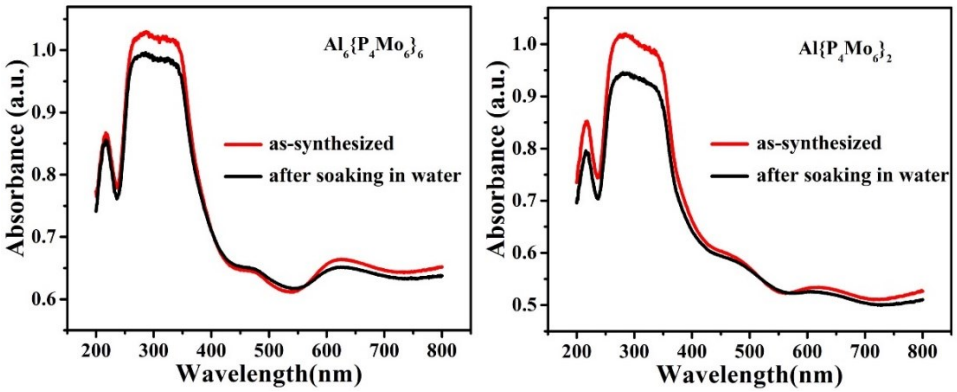

Figure S12. Solid UV-visible absorption spectra of $Al_6\{P_4Mo_6\}_6$ and $Al\{P_4Mo_6\}_2$ after immersing for 24 hours.

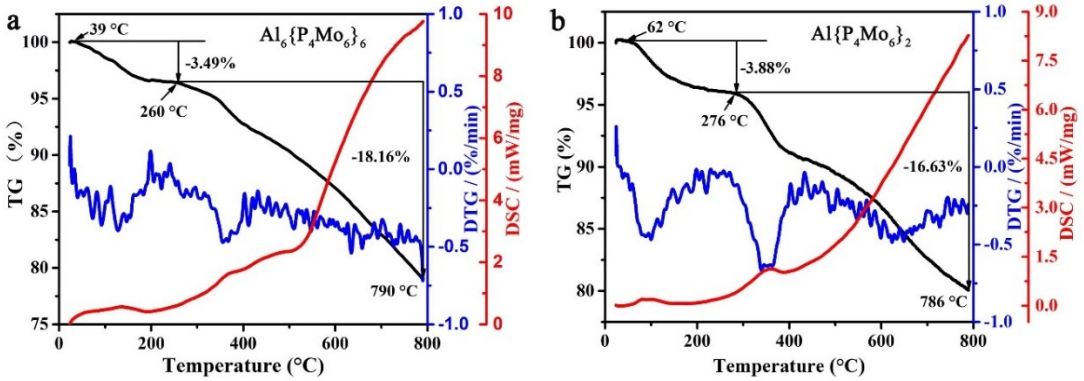

Figure S13. TG - DSC - DTG curves for crystals: (a) **$Al_6\{P_4Mo_6\}_6$**; (b) **$Al\{P_4Mo_6\}_2$**.

Thermogravimetric analyses of crystals **$Al_6\{P_4Mo_6\}_6$** and **$Al\{P_4Mo_6\}_2$** was carried out under a N_2 atmosphere from 20 to 800 ℃, and the TG curves are shown in Figure S13. The TG curve of **$Al_6\{P_4Mo_6\}_6$** displays two weight loss steps: the first weight loss of 3.49% (calc. 2.79%) in the temperature range of 29-260°C corresponds to the loss of lattice water and coordinated water molecules from Al(2) and Al(3); the second weight loss from 260-790°C is attributed to the decomposition of the bpe molecule (weight loss 18.16%, calc. 20.94%). The TG curves of **$Al\{P_4Mo_6\}_2$** also show two steps of weight loss: the first weight loss of 3.88% (calc. 3.77%) at 31-276°C corresponds to the loss of crystal waters; the second weight loss is attributed to the decomposition of the bpe molecule from 276-786°C (weight loss 16.63%, calc. 15.47%).

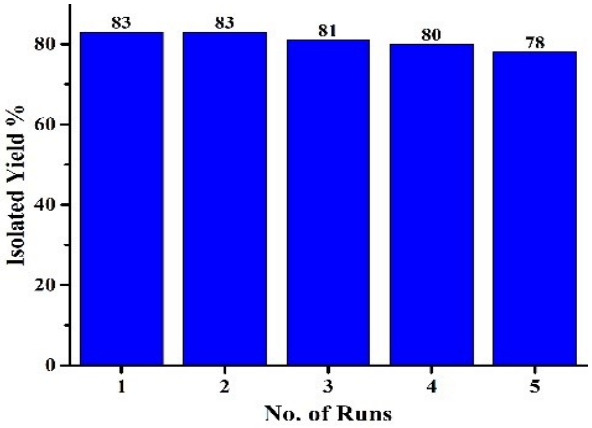

Figure S14. The recyclability of the **$Al_6\{P_4Mo_6\}_6$** towards catalytic reaction.

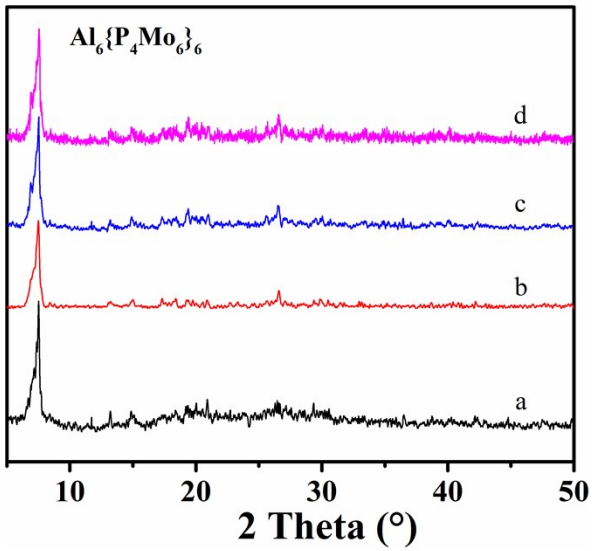

Figure S15. XRD comparison of the fresh **$Al_6\{P_4Mo_6\}_6$** (a) that after catalysis with three parallel experiments (b-d).

By comparing the XRD patterns of three parallel tests to the original data, it can be found that the intensities of peaks at 22° were basically unchanged and no new peaks were observed at 22°, while the intensities of peaks at 27° were slightly increased (Figure S15). As is known that the crystal grain size of sample could affect the diffraction intensity. It can be speculated that the slightly increased of peaks at 27° may be caused by the different grain size after catalytic reaction.

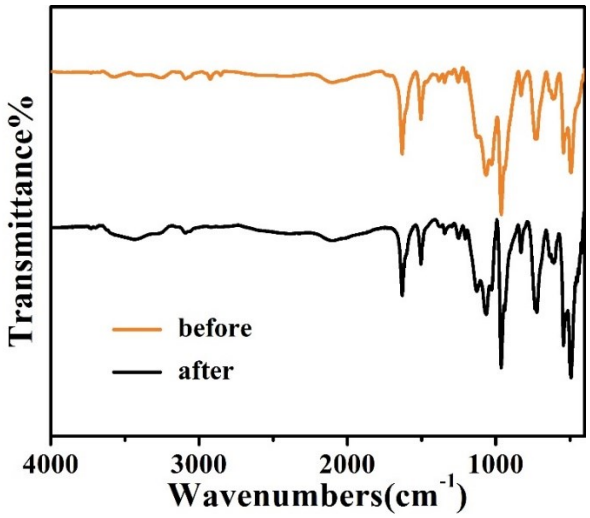

Figure S16. IR spectra comparison of **$Al_6\{P_4Mo_6\}_6$** between the fresh and after catalysis.

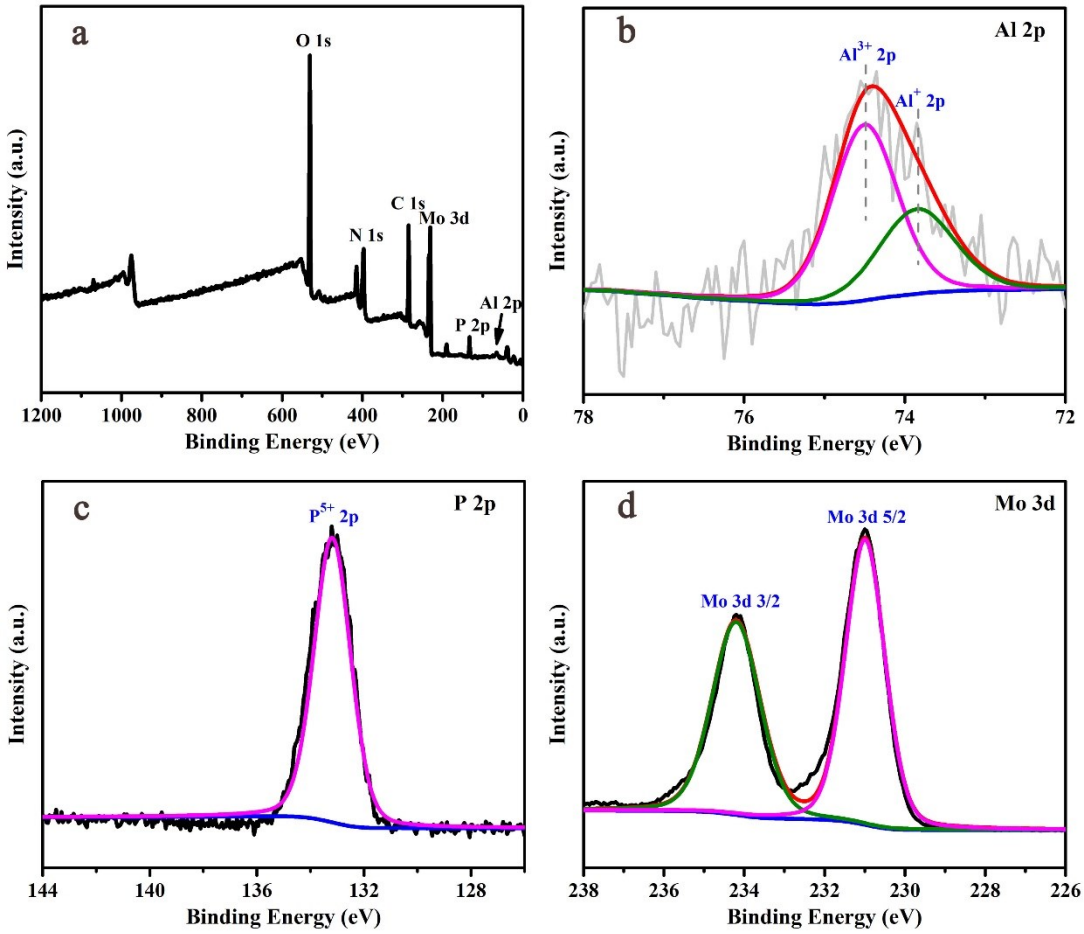

Figure S17. XPS spectra of **$Al_6\{P_4Mo_6\}_6$** after the catalytic reaction.

The XPS spectra of $Al_6\{P_4Mo_6\}_6$ after catalysis in Figure S17 show the existence of C, N, O, Al, Mo and P elements in $Al_6\{P_4Mo_6\}_6$. The high-resolution Al *2p* spectrum shows the presence of Al^{I} and Al^{III} with atomic ratio of *ca*. 1:1. The high-resolution Mo *3d* spectrum demonstrated the oxidation state of Mo atoms are +5. These results demonstrated that the structure of $Al_6\{P_4Mo_6\}_6$ after catalysis was kept.

Table S1. Crystal data and structural refinement details for hybrids **$Al_6\{P_4Mo_6\}_6$** and **$Al\{P_4Mo_6\}_2$**.

Hybrid	**$Al_6\{P_4Mo_6\}_6$**	**$Al\{P_4Mo_6\}_2$**
Empirical formula	C_{132} H_{200} Al_6 Mo_{36} N_{22} O_{201} P_{24}	C_{18} H_{33} $Al_{0.50}$ Mo_6 N_3 $O_{34.25}$ P_4
Formula weight	9670.13	1552.48
Crystal system	Monoclinic	Monoclinic
Space group	C2/c	P2(1)/c
a (Å)	48.173(5)	11.438(2)
b (Å)	13.8607(13)	23.034(4)
c (Å)	47.347(5)	15.788(3)
α, *β*, *γ* (°)	90, 117.571(3), 90	90, 95.203(3), 90
Volume ($Å^3$)	28024(5)	4142.3(13)
Z	4	4
Density(calculated)($Mg·m^{-3}$)	2.28	2.465
Absorption coefficient(mm^{-1})	1.824	2.042
$F_{(000)}$	18616.0	2958
Crystal size (mm^3)	0.2 × 0.19 × 0.18	0.300 × 0.260 × 0.240
ϑ (°)	0.970-24.984 °	1.568-25.008 °
Reflections collected	69187	20630
Independent reflections ($R_{(int)}$)	24556 [$R_{(int)}$ = 0.0330]	7293 [$R_{(int)}$ = 0.0241]
Data/restraints/parameters	24556 / 4044 / 1921	7293 / 1200 / 640
Goodness-of-fit on F^2	1.121	1.067
Final *R* indices [$I>2\sigma(I)$][a]	R_1 = 0.0596, wR_2 = 0.1437	R_1 = 0.0347, wR_2 = 0.0881
R indices (all data)	R_1 = 0.0688, wR_2 = 0.1489	R_1 = 0.0411, wR_2 = 0.0922

[a] $R_1 = \sum||F_0| - |F_c|| / \sum|F_0|$; $wR_2 = \{\sum[w(F_0^2 - F_c^2)^2] / \sum[w(F_0^2)^2]\}^{1/2}$.

Table S2. BVS calculations of Mo, P and Al centers in **$Al_6\{P_4Mo_6\}_6$** and **$Al\{P_4Mo_6\}_2$**.

	$Al_6\{P_4Mo_6\}_6$	$Al\{P_4Mo_6\}_2$
Mo1	5.080	5.389
Mo2	5.145	5.365
Mo3	5.185	5.367
Mo4	5.100	5.378
Mo5	5.134	5.395
Mo6	5.136	5.366
P1	4.815	4.939
P2	4.801	5.045
P3	4.777	4.975
P4	4.813	5.166
Al1	0.981	1.106
Al2	3.102	
Al3	3.112	
Al4	1.010	

Table S3. Selected bond lengths (Å) and bond angles (°) of **$Al_6\{P_4Mo_6\}_6$**.

Mo(1)-O(18)	1.964(6)	Mo(5)-O(27)	1.946(6)	P(3)-O(23)	1.911(6)
Mo(1)-O(20)	1.948(6)	Mo(5)-O(40)	2.085(7)	P(4)-O(61)	1.542(7)
Mo(2)-O(20)	1.954(6)	Mo(6)-O(12)	2.120(7)	P(5)-O(43)	1.593(7)
Mo(2)-O(35)	2.331(6)	Mo(6)-O(82)	2.082(6)	P(6)-O(63)	1.527(8)
Mo(3)-O(4)	1.958(6)	Al(1)-O(10)	2.308(7)	P(7)-O(81)	1.490(7)
Mo(3)-O(13)	1.941(6)	Al(2)-O(6)	1.911(6)	P(8)-O(1)	1.518(8)
Mo(4)-O(37)	1.948(6)	Al(3)-O(72)	1.900(6)	P(10)-O(93)	1.536(7)
Mo(4)-O(74)	1.678(7)	O(16) -Al(4)	2.273(6)	P(12)-O(14)	1.545(6)
O(18)-Mo(1)-O(23)	81.3(2)	O(4)-Mo(3)-O(11)	48.59(18)	O(26)-Al(1)-O(15)	98.8(2)
O(20)-Mo(1)-O(6)	103.2(2)	O(24)-Mo(3)-O(36)	79.2(2)	O(2W)-Al(3)-O(1W)	86.7(3)
O(25)-Mo(1)-O(18)	95.0(3)	O(13)-Mo(3)-Mo(11)	48.05(19)	O(83)-Al(3)-O(81)	94.0(3)
O(23)-Mo(1)-Mo(2)	87.93(16)	O(35)-P(3)-O(23)	107.8(3)	O(18)-Al(4)-O(16)	98.7(2)
O(20)-Mo(2)-O(35)	83.5(2)	O(81)-P(7)-O(94)	107.7(4)	Mo(1)-O(54)-Mo(11)	112.9(3)
O(44)-Mo(2)-O(35)	71.6(2)	O(6)-Al(2)-O(3W)	85.7(3)	Mo(6)-O(26)-Al(1)	131.1(3)
O(47)-Mo(2)-O(77)	96.2(3)	O(6)#1-Al(2)-O(3W)	87.0(3)	P(1)-O(6)-Al(2)	135.9(4)
O(77)-Mo(2)-Mo(1)	135.3(2)	O(5)-Al(1)-O(9)	96.9(2)	Mo(2)-O(18)-Al(4)	132.5(3)

Symmetry transformations used to generate equivalent atoms: #1 1-x, y, -z+1/2.

Table S4. Selected bond lengths (Å) and bond angles (°) of **Al{P_4Mo_6}$_2$**.

Mo(1)-O(7)	1.667(4)	Al(1)-O(2)	2.267(3)	P(3)-O(16)	1.503(4)
Mo(2)-O(10)	1.664(4)	Al(1)-O(2)#1	2.267(3)	P(3)-O(13)	1.528(4)
Mo(3)-O(21)	1.657(4)	Al(1)-O(5)	2.277(4)	P(4)-O(18)	1.510(5)
Mo(4)-O(15)	1.667(4)	Al(1)-O(5)#1	2.277(4)	P(4)-O(29)	1.487(5)
Mo(5)-O(25)	2.056(4)	Al(1)-O(3)	2.286(4)	Mo(5)-O(2)	1.928(3)
Mo(6)-O(27)	2.048(4)	Al(1)-O(3)#1	2.287(4)	Mo(5)-O(17)	1.925(4)
Mo(1)-Mo(6)	2.5628(7)	P(1)-O(8)	1.518(4)	Mo(6)-O(3)	1.934(4)
Mo(2)-Mo(3)	2.5816(7)	P(2)-O(25)	1.479(5)	Mo(5)-O(28)	2.347(4)
O(7)-Mo(1)-O(17)	105.70(19)	O(14)-Mo(5)-O(25)	86.10(19)	O(18)-Mo(4)-Mo(5)	134.97(13)
O(7)-Mo(1)-O(3)	102.67(17)	O(20)-Mo(5)-O(11)	99.37(19)	O(2)-Al(1)-O(2)#1	180.0
O(17)-Mo(1)-O(3)	95.20(15)	O(17)-Mo(6)-O(3)	95.23(16)	O(5)-Al(1)-O(5)#1	180.0
O(1)-Mo(2)-O(4)	155.22(15)	O(24)-Mo(6)-O(27)	98.1(2)	O(2)-Al(1)-O(3)#1	83.63(13)
O(13)-Mo(2)-O(6)	80.27(14)	O(7)-Mo(1)-Mo(6)	101.38(14)	O(5)-Al(1)-O(3)#1	97.10(13)
O(1)-Mo(3)-O(5)	95.19(15)	O(3)-Mo(1)-Mo(6)	48.50(11)	Mo(2)-O(5)-Mo(3)	83.51(14)
O(21)-Mo(3)-O(5)	102.33(19)	O(1)-Mo(2)-Mo(3)	48.11(11)	Mo(3)-O(5)-Al(1)	132.91(18)
O(15)-Mo(4)-O(2)	102.11(18)	O(6)-Mo(2)-Mo(3)	89.20(9)	P(1)-O(6)-Mo(2)	126.5(2)
O(15)-Mo(4)-O(8)	170.26(18)	O(26)-Mo(3)-Mo(2)	133.14(12)	P(2)-O(26)-Mo(3)	134.4(3)

Symmetry transformations used to generate equivalent atoms: #1 1-x, 1-y, -z.

Table S5. The XPS result of **$Al_6\{P_4Mo_6\}_6$** and **$Al\{P_4Mo_6\}_2$**.

Hybrid	Name	Atom %
$Al_6\{P_4Mo_6\}_6$	C1s	41.2
	N1s	18.02
	O1s	26.75
	P2p	5.27
	Al2p	1.63
	Mo3d	5.95
$Al\{P_4Mo_6\}_2$	C1s	48.64
	N1s	16.31
	O1s	23.78
	P2p	4.36
	Al2p	1.41
	Mo3d	4.53

Table S6. The ICP result of **$Al_6\{P_4Mo_6\}_6$** and **$Al\{P_4Mo_6\}_2$**.

Hybrid	Theoretical Al content (μg/mL)	Actual Al content (μg/mL)
$Al_6\{P_4Mo_6\}_6$	5.00	5.183963
	2.50	2.445948
$Al\{P_4Mo_6\}_2$	1.00	1.043829

Table S7. Substrate scope for the $Al_6\{P_4Mo_6\}_6$ catalyzed one-pot four-component domino reaction [a].

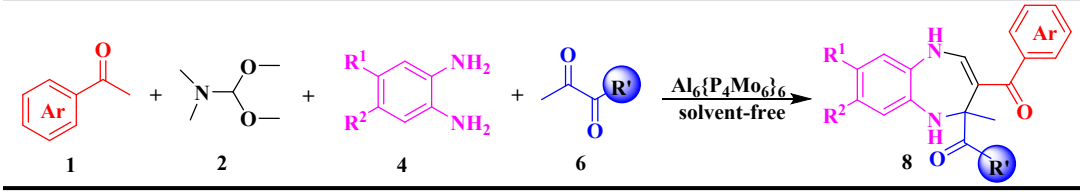

Entry	Aromatic ketones	1,2-phenylenediamines	Ketones derivatives	Product	Yield[b] (%)
1	Ph	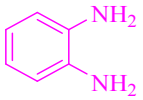	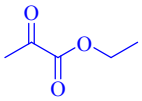	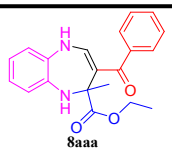 8aaa	86
2	Ph	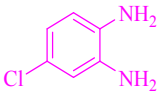	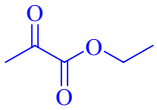	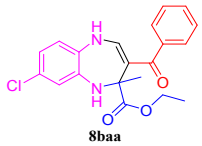 8baa	76
3	Ph	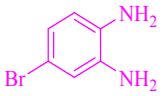	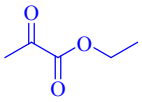	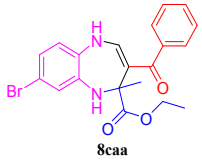 8caa	79
4	Ph	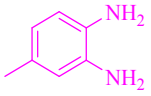	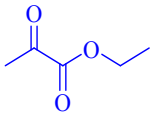	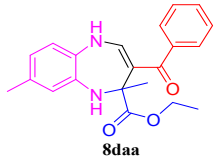 8daa	88
5	Ph	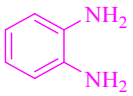	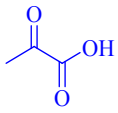	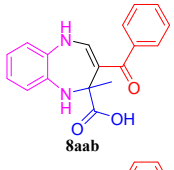 8aab	78
6	Ph	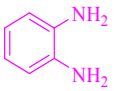	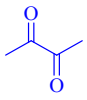	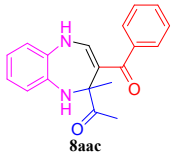 8aac	82
7	4-ClPh	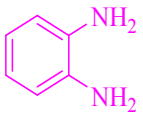	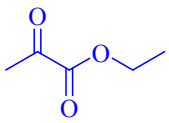	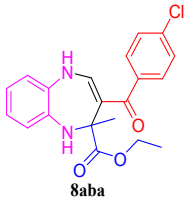 8aba	86
8	4-CH_3Ph	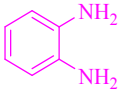	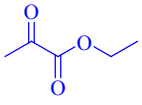	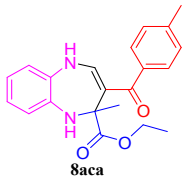 8aca	78

9	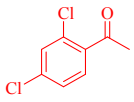	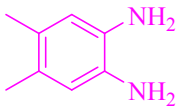	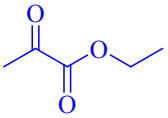	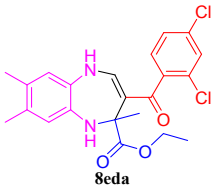	90

[a] Reaction conditions: aromatic ketones 1 (1.00 mmol), *N,N*-dimethylformamide dimethyl acetal 2 (1.00 mmol), 1,2-phenylenediamines 4 (1.00 mmol), ketone derivatives 6 (1.00 mmol) and catalyst (10.00 mg).[b] Isolated yield when the reaction was performed at 30 °C, under solvent free reaction conditions, 20 min.

Physical characterization data of the synthesized compounds.

Ethyl 3-benzoyl-2-methyl-2,5-dihydro-1*H*-benzo[*b*][1,4]diazepine-2-carboxylate **8aaa**

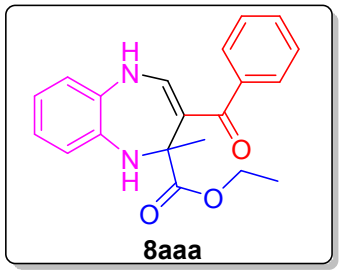

8aaa

Yield: 86%;
Characteristic: Light yellow solid;
M.p.: 218–219 °C;
IR (KBr): 3346, 3301, 1724, 1639, 1588 cm^{-1};
^1H NMR(400 MHz, DMSO-d_6, TMS): δ 0.90 (3H, t, *J*=8.0 Hz, Me), 1.58 (3H, s, Me), 3.92 (2H, q, *J*=8.0Hz, CH_2), 5.64 (1H, s, NH), 6.79-6.92 (4H, m, Ph), 7.03 (1H, d, *J*=8.0Hz, CH), 7.43-7.52 (5H, m, Ph), 9.33 (1H, d, *J*=8.0Hz, NH);
^{13}C NMR (100 MHz, DMSO-d_6, TMS): δ 14.29, 25.64, 60.32, 63.21, 116.56, 119.47, 121.65, 122.42, 123.39, 128.62, 130.52, 132.53, 137.12, 140.93, 144.19, 172.61, 194.04;
MS calcd for $C_{20}H_{20}N_2O_3$ 336, found 337 (M + 1);
anal. calcd (%) for $C_{20}H_{20}N_2O_3$: C 71.41, H 5.99, N 8.33; found: C 71.70, H 6.01, N 8.30.
Ethyl 3-benzoyl-8-chloro-2-methyl-2,5-dihydro-1*H*-benzo[*b*][1,4]diazepine-2-carboxylate **8baa**

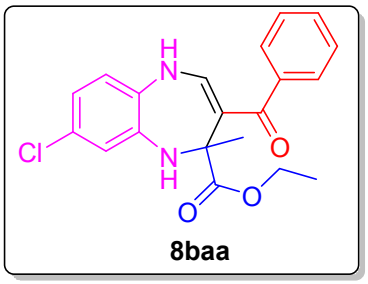

8baa

Yield: 76%;

Characteristic: Off-white solid;
M.p.: 253–255 °C;
IR (KBr): 3353, 3295, 1724, 1646, 1548;
^{1}H NMR(400 MHz, DMSO-d_6, TMS): δ 0.96 (3H, t, J=8.0 Hz, Me), 1.62 (3H, s, Me), 3.98 (2H, q, J=8.0Hz, CH_2), 5.98 (1H, s, NH), 6.88-6.93 (3H, m, Ph), 7.16 (1H, d, J=4.0Hz, CH), 7.49-7.54 (5H, m, Ph), 9.45 (1H, d, J=4.0Hz, NH);
^{13}C NMR (100 MHz, DMSO-d_6, TMS): δ 14.39, 25.46, 60.47, 63.20, 116.51, 120.80, 121.09, 121.34, 126.59, 128.65, 128.78, 130.70, 131.46, 138.43, 140.65, 143.56, 172.29, 194.16;
MS calcd for $C_{20}H_{19}ClN_2O_3$ 370, found 371 (M + 1);
anal. calcd (%) for $C_{20}H_{19}ClN_2O_3$: C 64.78, H 5.16, N 7.55; found: C 64.92, H 5.18, N 7.56.
Ethyl 3-benzoyl-8-bromo-2-methyl-2,5-dihydro-1*H*-benzo[*b*][1,4]diazepine-2-carboxylate **8caa**

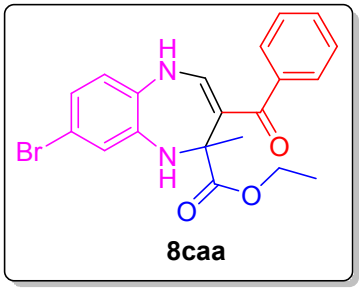

8caa

Yield: 79%;
Characteristic: Gray solid;
M.p.: 231–232 °C;
IR (KBr): 3353, 3295, 1717, 1646, 1569;
^{1}H NMR(400 MHz, DMSO-d_6, TMS): δ 0.95 (3H, t, J=8.0 Hz, Me), 1.61 (3H, s, Me), 3.97 (2H, q, J=8.0Hz, CH_2), 5.97 (1H, s, NH), 6.80-7.01 (3H, m, Ph), 7.28 (1H, d, J=4.0Hz, CH), 7.49-7.54 (5H, m, Ph), 9.45 (1H, d, J=4.0Hz, NH);
^{13}C NMR (100 MHz, DMSO-d_6, TMS): δ 14.39, 25.43, 60.47, 63.19, 114.46, 116.56, 121.13, 123.95, 124.17, 128.66, 128.79, 130.73, 131.88, 138.73, 140.62, 143.51, 172.26, 194.16;
MS calcd for $C_{20}H_{19}BrN_2O_3$ 414, found 415 (M + 1);
anal. calcd (%) for $C_{20}H_{19}BrN_2O_3$: C 57.84, H 4.61, N 6.75; found: C 58.09, H 4.62, N 6.73.
Ethyl 3-benzoyl-2,8-dimethyl-2,5-dihydro-1*H*-benzo[*b*][1,4]diazepine-2-carboxylate **8daa**

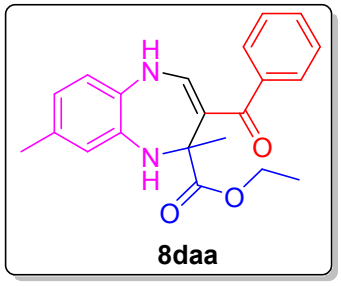

8daa

Yield: 88%;
Characteristic: Light yellow solid;
M.p.: 175–176 °C;
IR (KBr): 3359, 3295, 1724, 1633, 1543;
^{1}H NMR(400 MHz, DMSO-d_6, TMS): δ 0.98 (3H, t, J=8.0 Hz, Me), 1.61 (3H, s, Me), 2.22 (3H, s, Me), 3.98 (2H, q, J=8.0Hz, CH_2), 5.58 (1H, s, NH), 6.67-6.88 (3H, m, Ph), 6.93 (1H, d, J=8.0Hz, CH),

7.52-7.53 (5H, m, Ph), 9.33 (1H, d, *J*=8.0Hz, NH); ^{13}C NMR (100 MHz, DMSO-d_6, TMS): δ 14.30, 20.74, 25.73, 60.28, 63.19, 116.24, 119.44, 122.31, 122.73, 128.61, 130.09, 130.41, 132.38, 136.97, 141.05, 144.28, 172.60, 193.82;
MS calcd for $C_{21}H_{22}N_2O_3$ 350, found 351 (M + 1);
anal. calcd (%) for $C_{21}H_{22}N_2O_3$: C 71.98, H 6.33, N 7.99; found: C 72.14, H 6.35, N 8.01.
Ethyl 3-benzoyl-2,7,8-trimethyl-2,5-dihydro-1*H*-benzo[*b*][1,4]diazepine-2-carboxylate **8eaa**

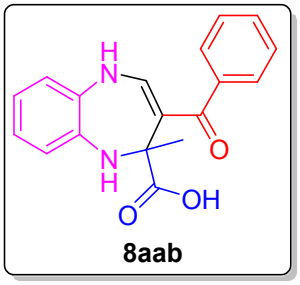

8aab

Yield: 78%;
Characteristic: Yellow solid;
M.p.: 180–182 °C;
IR (KBr): 3372, 3269, 1710, 1620, 1594;
^{1}H NMR(400 MHz, DMSO-d_6, TMS): δ 1.56 (3H, s, Me), 5.57 (1H, s, NH), 6.78-6.88 (4H, m, Ph), 7.03 (1H, d, *J*=8.0Hz, CH), 7.44-7.52 (5H, m, Ph), 9.29 (1H, d, *J*=8.0Hz, NH), 11.97 (1H, s, COOH);
^{13}C NMR (100 MHz, DMSO-d_6, TMS): δ 25.70, 63.32, 116.61, 119.39, 121.39, 122.44, 123.30, 128.62, 128.86, 130.58, 132.28, 137.35, 141.06, 144.08, 174.10, 194.28;
MS calcd for $C_{18}H_{16}N_2O_3$ 308, found 309 (M + 1);
anal. calcd (%) for $C_{18}H_{16}N_2O_3$: C 70.12 H 5.23, N 9.09; found: C 70.39, H 5.25, N 9.11.

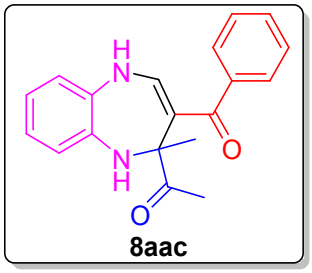

8aac

Yield: 82%;
Characteristic: Light yellow solid;
M.p.: 232–234 °C;
IR (KBr): 3301, 3185, 1717, 1620, 1491;
^{1}H NMR(400 MHz, DMSO-d_6, TMS): δ 1.37 (3H, s, Me), 2.00 (3H, s, Me), 5.53 (1H, s, NH), 6.81-6.88 (4H, m, Ph), 7.37 (1H, d, *J*=8.0Hz, CH), 7.36-7.52 (5H, m, Ph), 9.56 (1H, d, *J*=8.0Hz, NH);
^{13}C NMR (100 MHz, DMSO-d_6, TMS): δ 21.87, 25.00, 66.97, 117.05, 119.98, 121.37, 122.41, 123.84, 128.41, 128.55, 128.65, 130.34, 131.37, 134.99, 137.45, 140.82, 145.78, 193.54, 204.22;
MS calcd for $C_{19}H_{18}N_2O_2$ 306, found 307 (M + 1);
anal. calcd (%) for $C_{19}H_{18}N_2O_2$: C 74.49, H 5.92, N 9.14; found: C 74.69, H 5.91, N 9.16.
Ethyl 3-(2,4-dichlorobenzoyl)-2,7,8-trimethyl-2,5-dihydro-1*H*-benzo[*b*][1,4]diazepine-2-carboxylate **8eda**

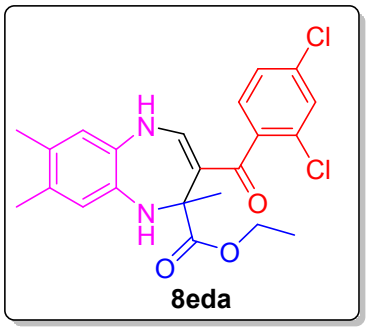

8eda

Yield: 90%;
Characteristic: Light yellow solid;
M.p.: 245–246 °C;
IR (KBr): 3340, 3289, 1724, 1639, 1581;
^{1}H NMR(400 MHz, DMSO-d_6, TMS): δ 1.04 (3H, t, J=8.0 Hz, Me), 1.51 (3H, s, Me), 2.08 (6H, s, Me), 3.91 (2H, q, J=8.0Hz, CH_2), 5.39 (1H, s, NH), 6.61 (1H, s, Ph), 6.81 (1H, s, Ph), 6.64-7.69 (3H, m, Ph), 7.29 (1H, d, J=8.0Hz, CH), 9.38 (1H, d, J=8.0Hz, NH);
^{13}C NMR (100 MHz, DMSO-d_6, TMS): δ 14.48, 18.90, 19.25, 25.81, 60.41, 63.66, 116.69, 120.85, 123.87, 127.82, 129.41, 129.48, 129.75, 130.54, 131.66, 131.90, 134.16, 135.07, 139.45, 146.09, 172.34, 189.01;
MS calcd for $C_{22}H_{22}Cl_2N_2O_3$ 432, found 433 (M + 1);
anal. calcd (%) for $C_{22}H_{22}Cl_2N_2O_3$: C 66.24, H 5.81, N 7.02; found: C 66.52, H 5.82, N 7.01.

Ethyl 2-methyl-3-(4-methylbenzoyl)-2,5-dihydro-1*H*-benzo[*b*][1,4]diazepine-2-carboxylate **8aca**

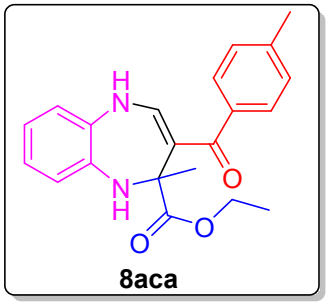

8aca

Yield: 78%;
Characteristic: White solid;
M.p.: 234–235 °C;
IR (KBr): 3372, 3295, 1724, 1639, 1607;
^{1}H NMR(400 MHz, DMSO-d_6, TMS): δ 0.87 (3H, t, J=8.0 Hz, Me), 1.54 (3H, s, Me), 2.36 (3H, s, Me), 3.89 (2H, q, J=8.0Hz, CH_2), 5.61 (1H, s, NH), 6.81-6.89 (4H, m, Ph), 6.99 (1H, d, J=8.0Hz, CH), 7.25-7.42 (4H, m, Ph), 9.25 (1H, d, J=8.0Hz, NH); ^{13}C NMR (100 MHz, DMSO-d_6, TMS): δ 14.43，21.31 25.58, 60.26, 63.13, 116.53, 119.37, 121.59, 122.36, 123.24, 128.95, 129.12, 132.59, 137.07, 138.04, 140.41, 143.65, 172.64, 194.00;
MS calcd for $C_{21}H_{22}N_2O_3$ 350, found 351 (M + 1);
anal. calcd (%) for $C_{21}H_{22}N_2O_3$: C 71.98, H 6.33, N 7.99; found: C 72.73, H 6.31, N 8.00.
Ethyl 3-(4-chlorobenzoyl)-2-methyl-2,5-dihydro-1*H*-benzo[*b*][1,4]diazepine-2-carboxylate **8aba**

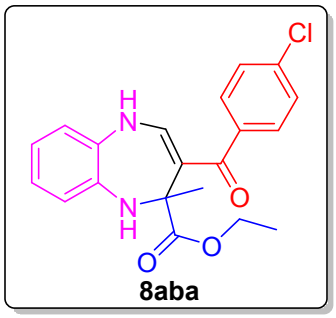

8aba

Yield: 86%;
Characteristic: White solid;
M.p.: 230–231 °C;
IR (KBr): 3359, 3301, 1730, 1639, 1581;
^{1}H NMR(400 MHz, DMSO-d_6, TMS): δ 0.92 (3H, t, J=8.0 Hz, Me), 1.57 (3H, s, Me), 3.92 (2H, q, J=8.0Hz, CH_2), 5.69 (1H, s, NH), 6.82-6.89 (4H, m, Ph), 7.04 (1H, d, J=8.0Hz, CH), 7.56 (4H, m, Ph), 9.40 (1H, d, J=8.0Hz, NH);
^{13}C NMR (100 MHz, DMSO-d_6, TMS): δ 14.30, 25.53, 60.34, 63.16, 116.38, 119.57, 121.65, 122.41, 123.52, 128.73, 130.64, 132.38, 135.29, 137.15, 139.59, 144.27, 172.50, 192.65;
MS calcd for $C_{20}H_{19}ClN_2O_3$ 370, found 371 (M + 1);
anal. calcd (%) for $C_{20}H_{19}ClN_2O_3$: C 64.78, H 5.16, N 7.55; found: C 65.09, H 5.15, N 7.54.

[1]HNMR & [13]CNMR & IR and MS Spectra of the synthesized compounds

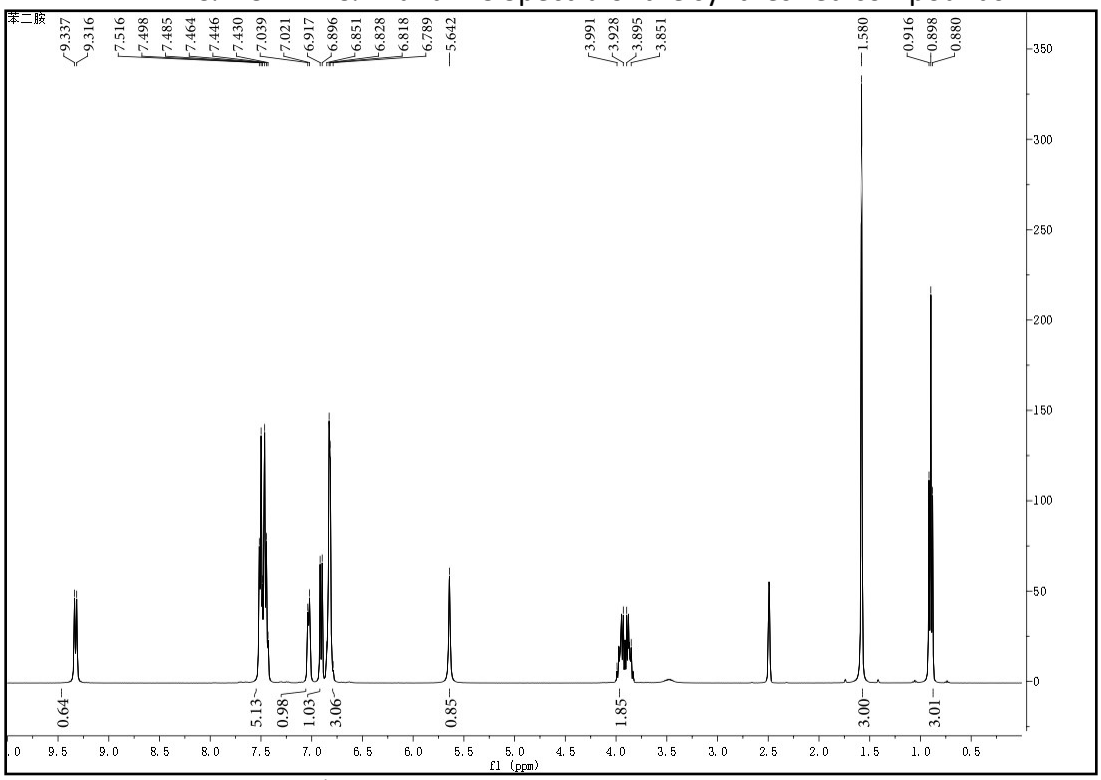

[1]H NMR spectra of compound **8aaa**

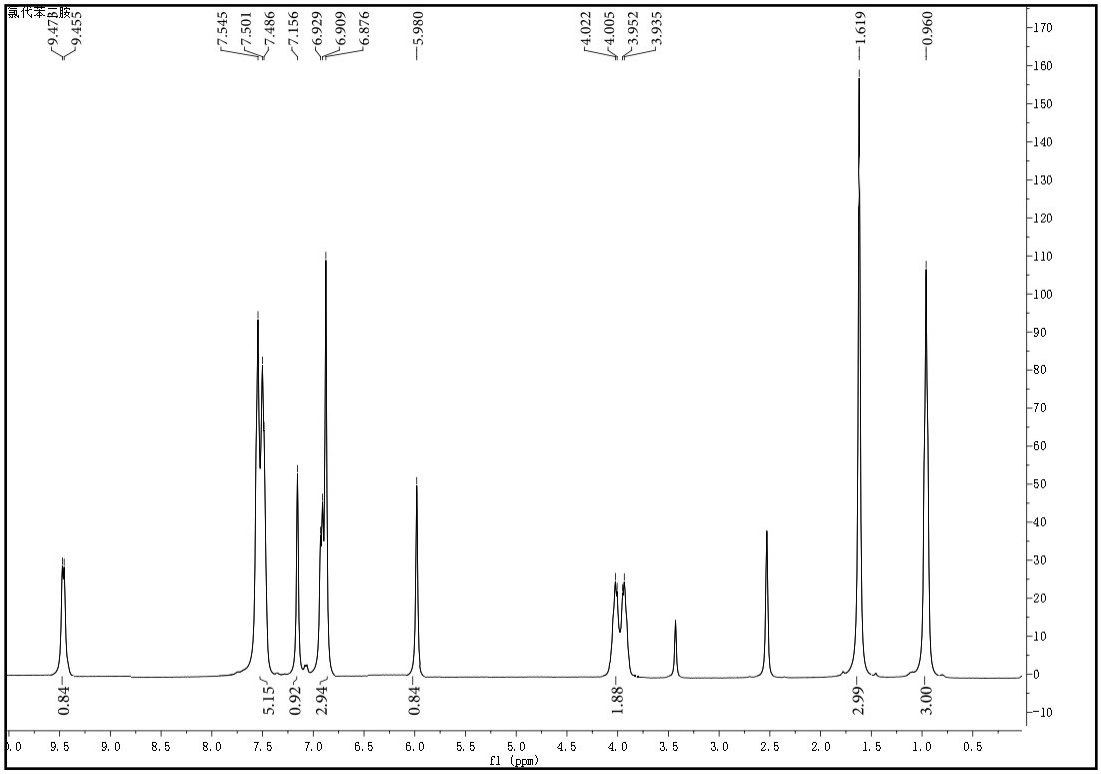

[1]H NMR spectra of compound **8baa**

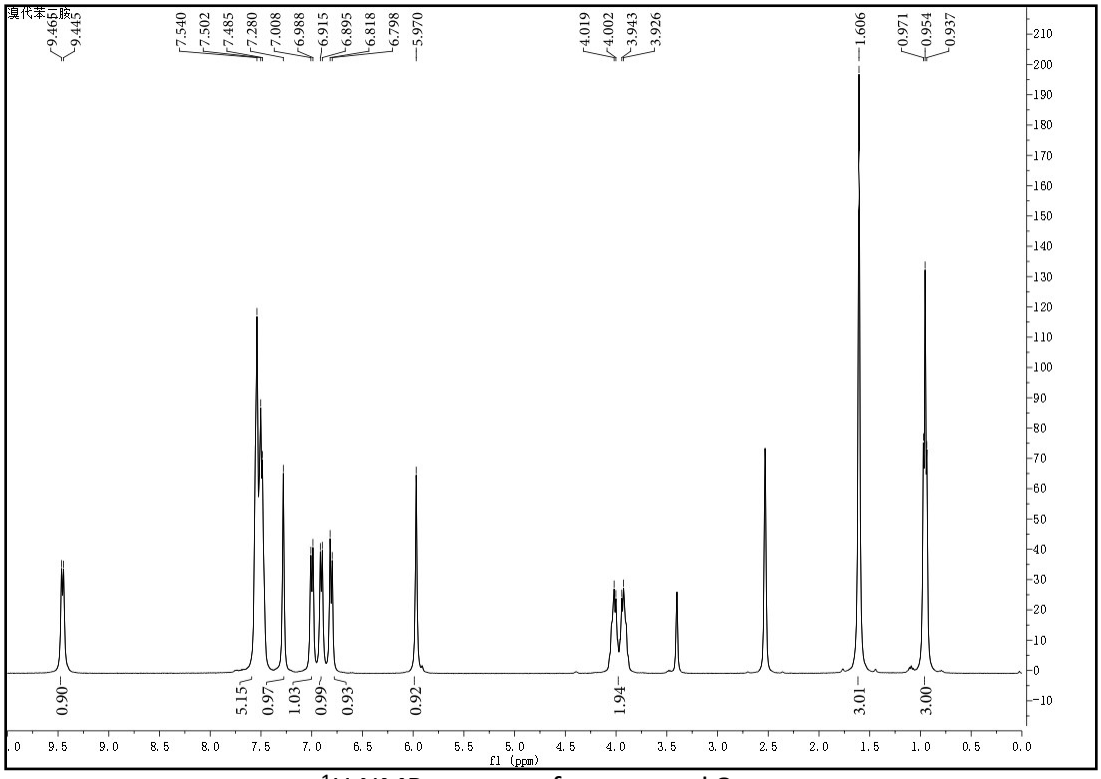

^{1}H NMR spectra of compound **8caa**

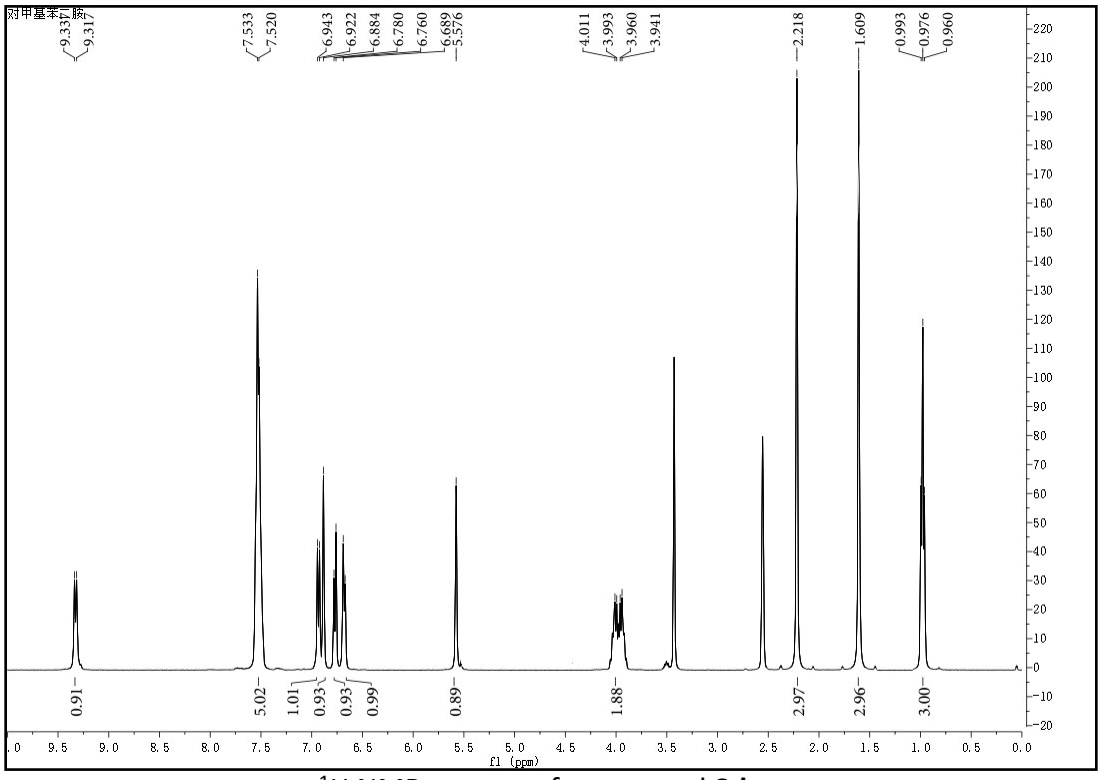

^{1}H NMR spectra of compound **8daa**

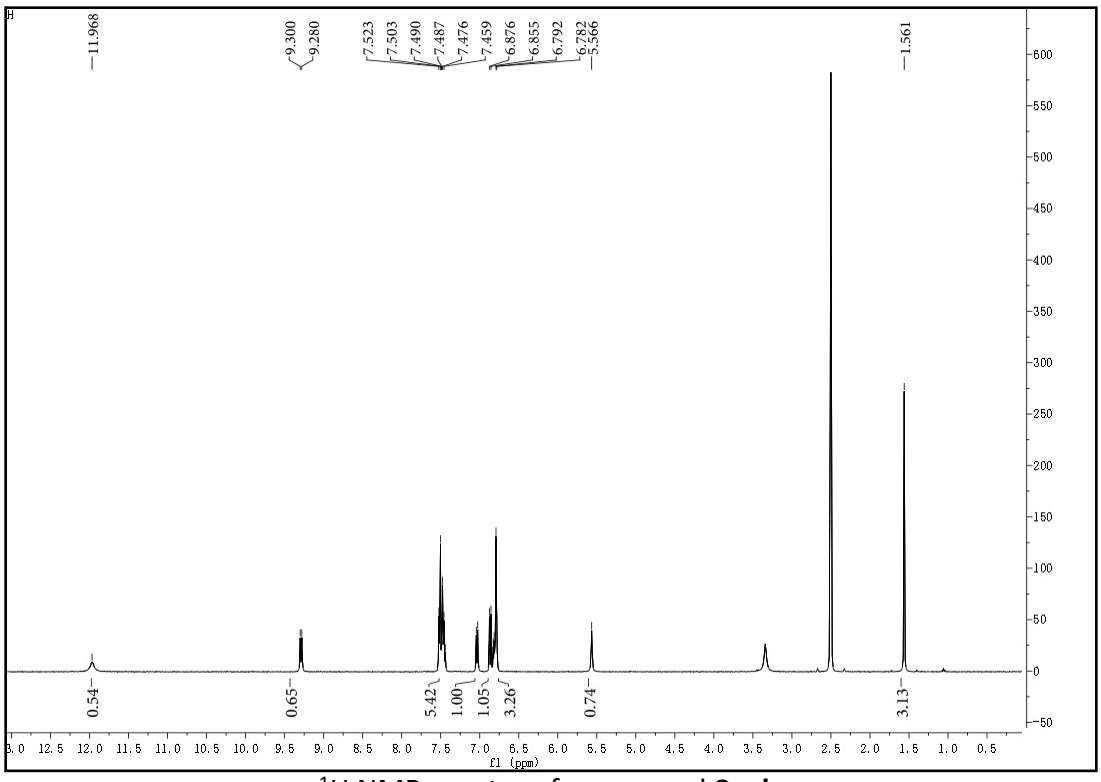

^{1}H NMR spectra of compound **8aab**

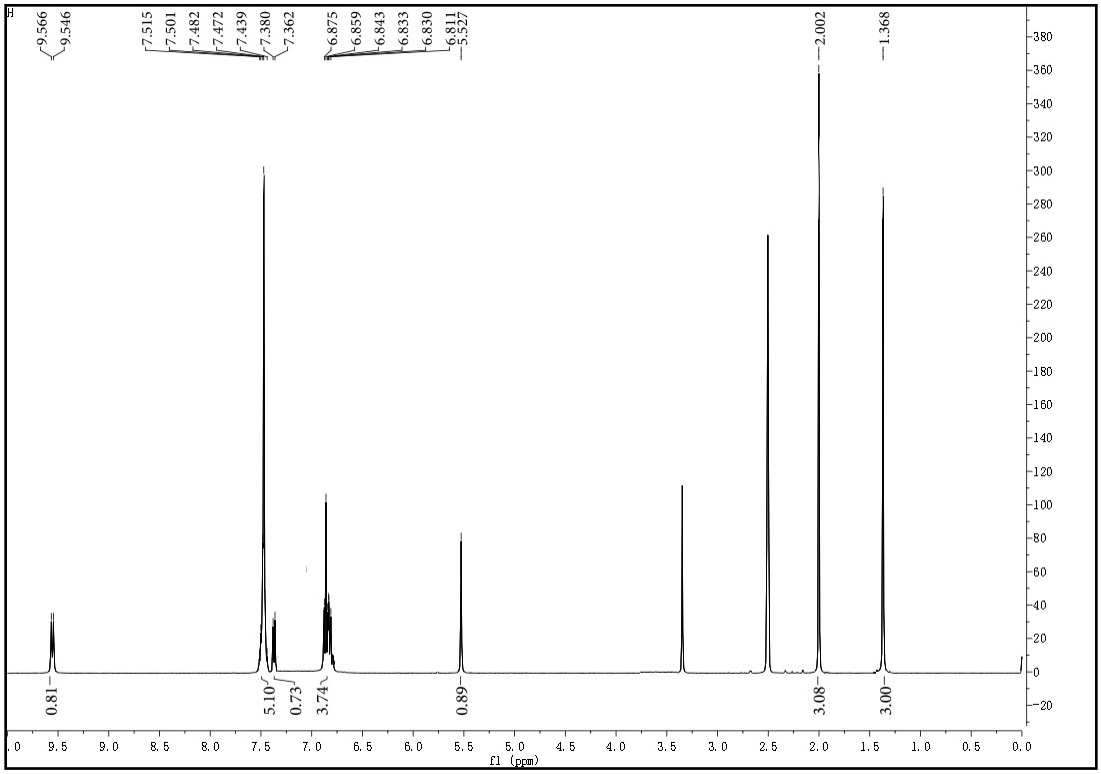

^{1}H NMR spectra of compound **8aac**

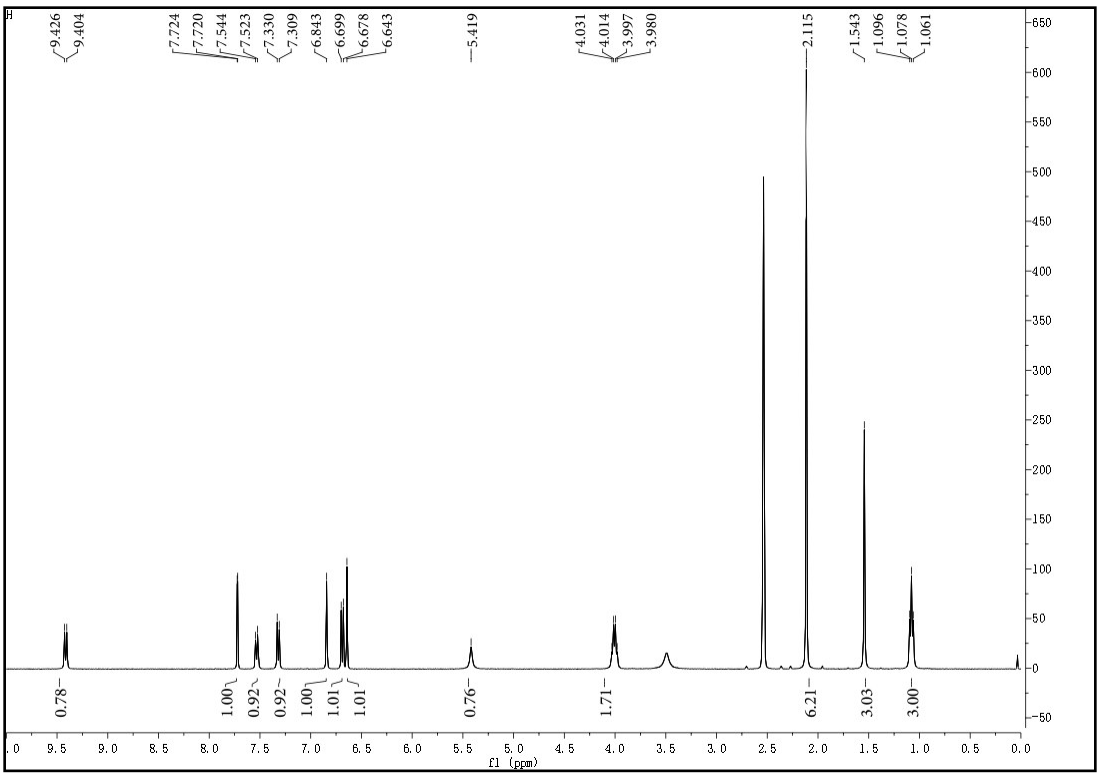

^{1}H NMR spectra of compound **8eda**

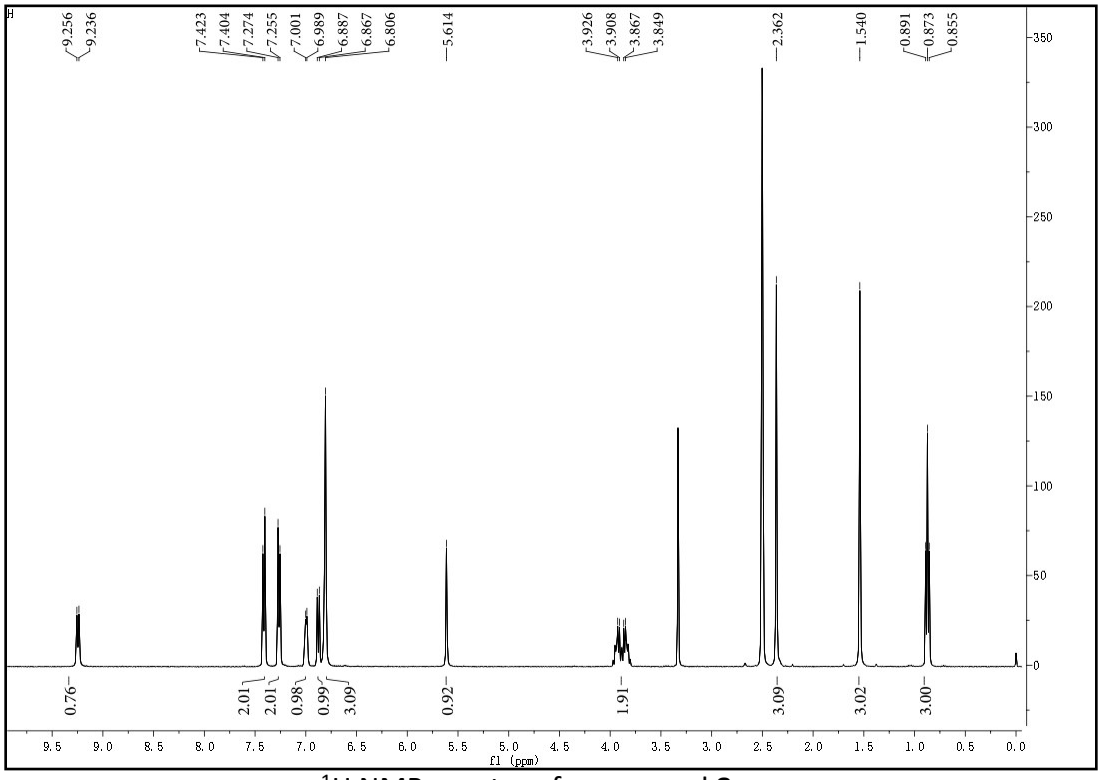

^{1}H NMR spectra of compound **8aca**

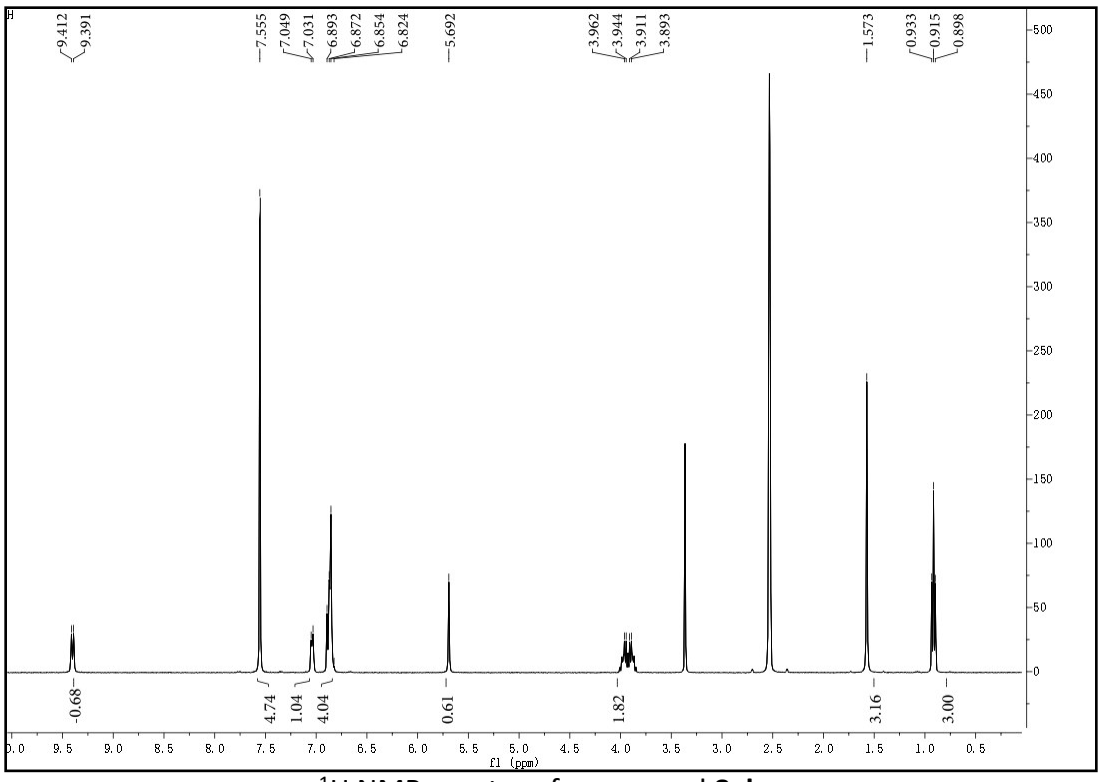

^{1}H NMR spectra of compound **8aba**

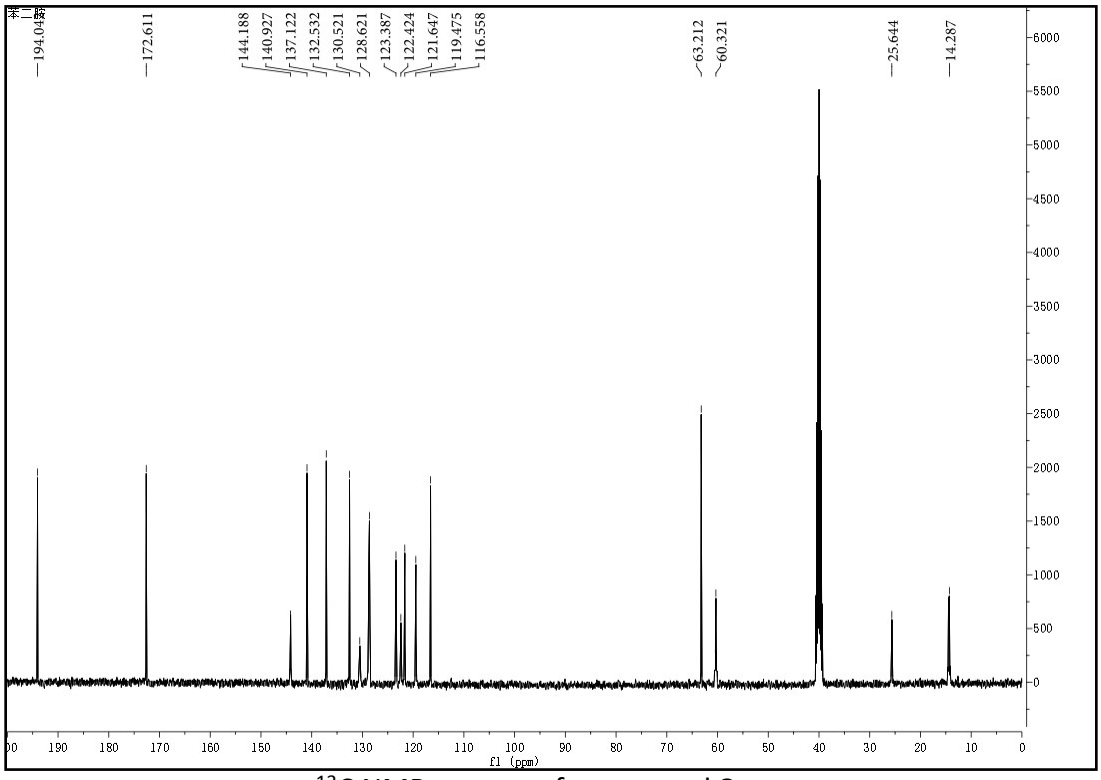

^{13}C NMR spectra of compound **8aaa**

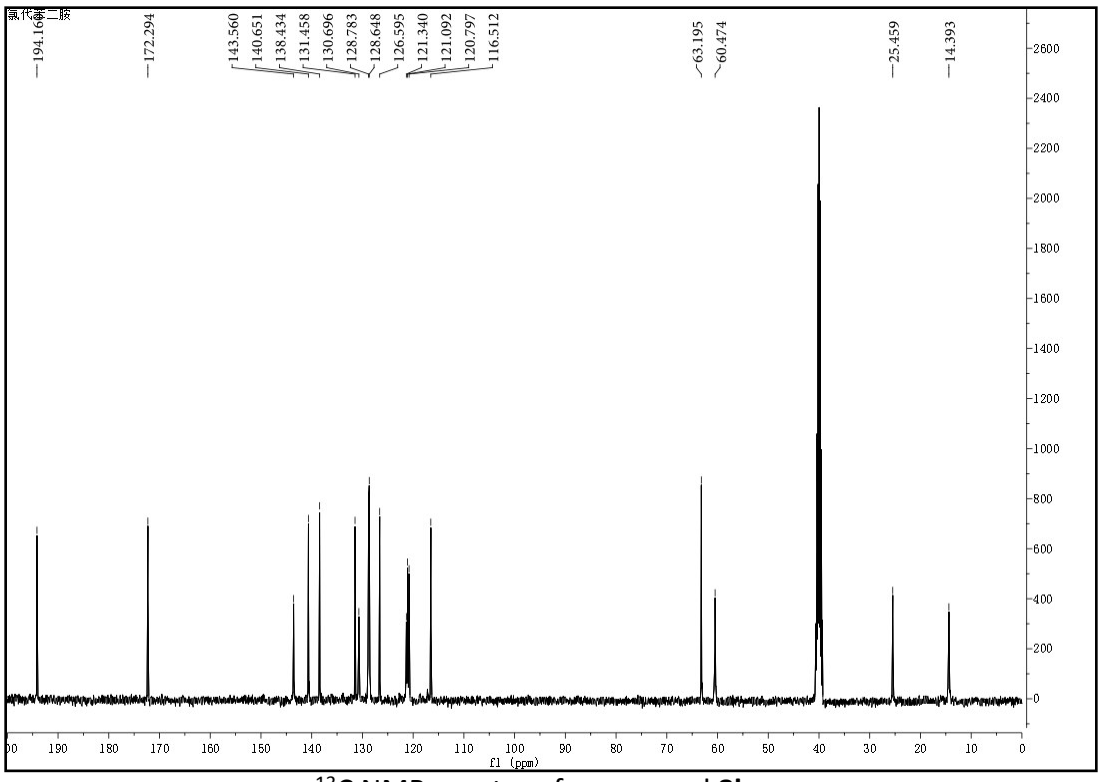

^{13}C NMR spectra of compound **8baa**

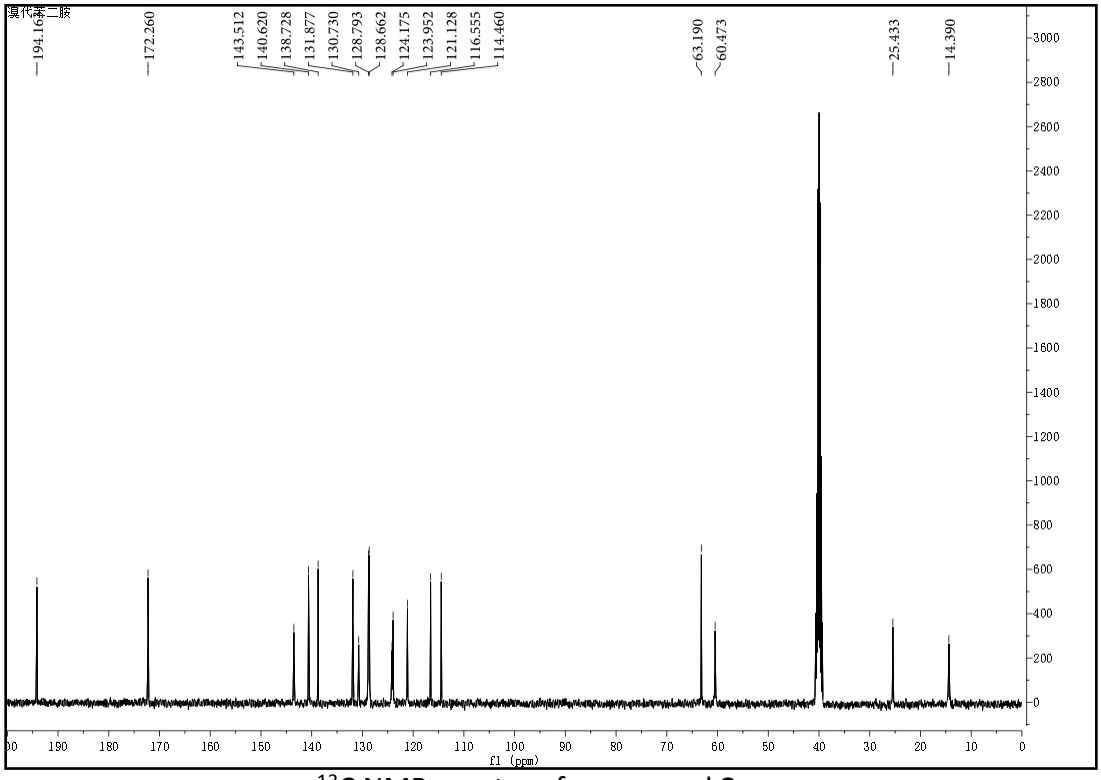

^{13}C NMR spectra of compound **8caa**

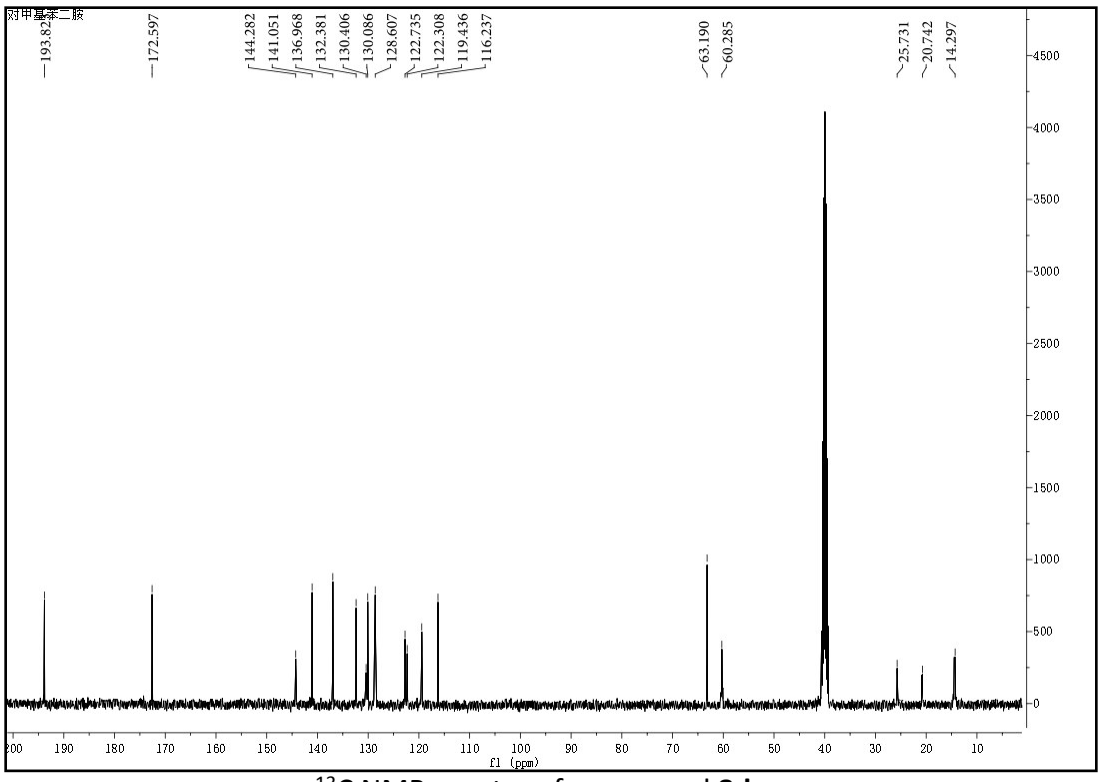

^{13}C NMR spectra of compound **8daa**

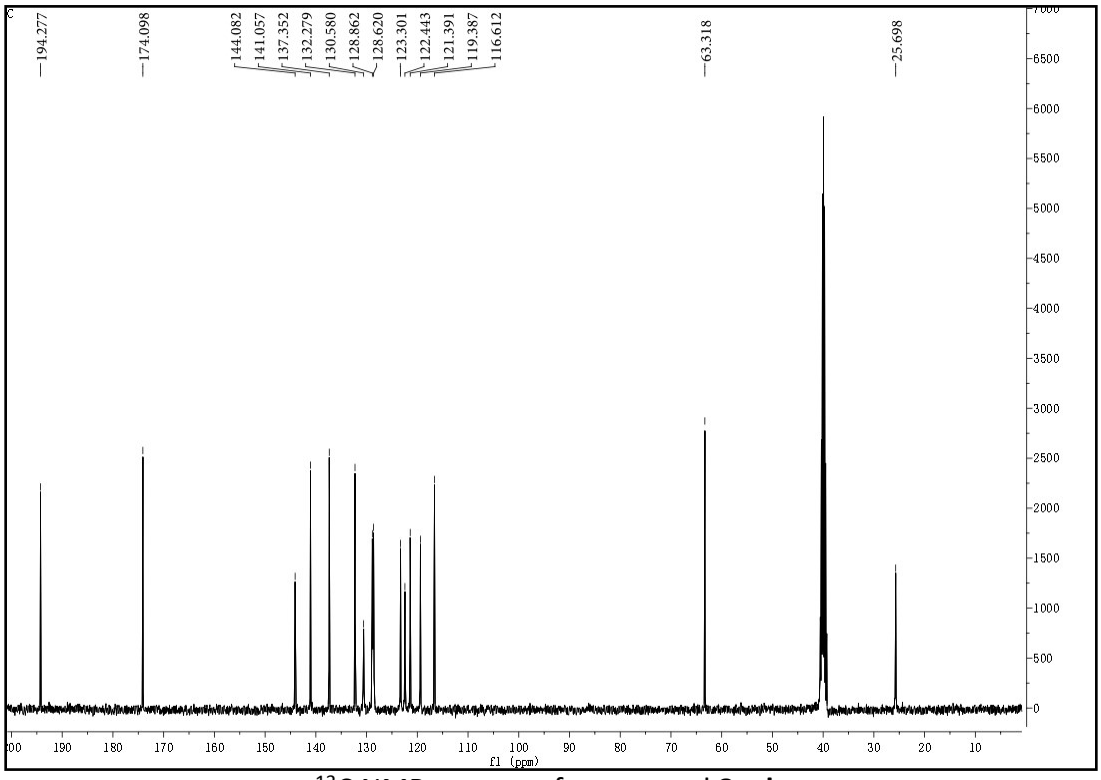

^{13}C NMR spectra of compound **8aab**

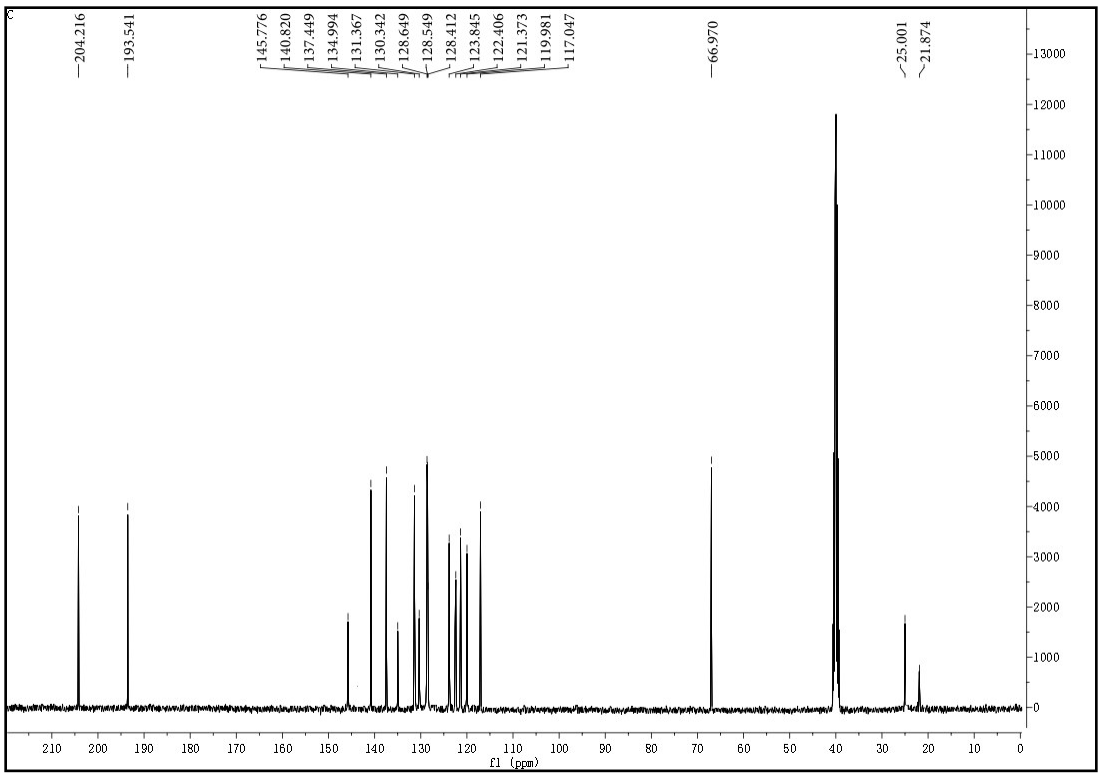

^{13}C NMR spectra of compound **8aac**

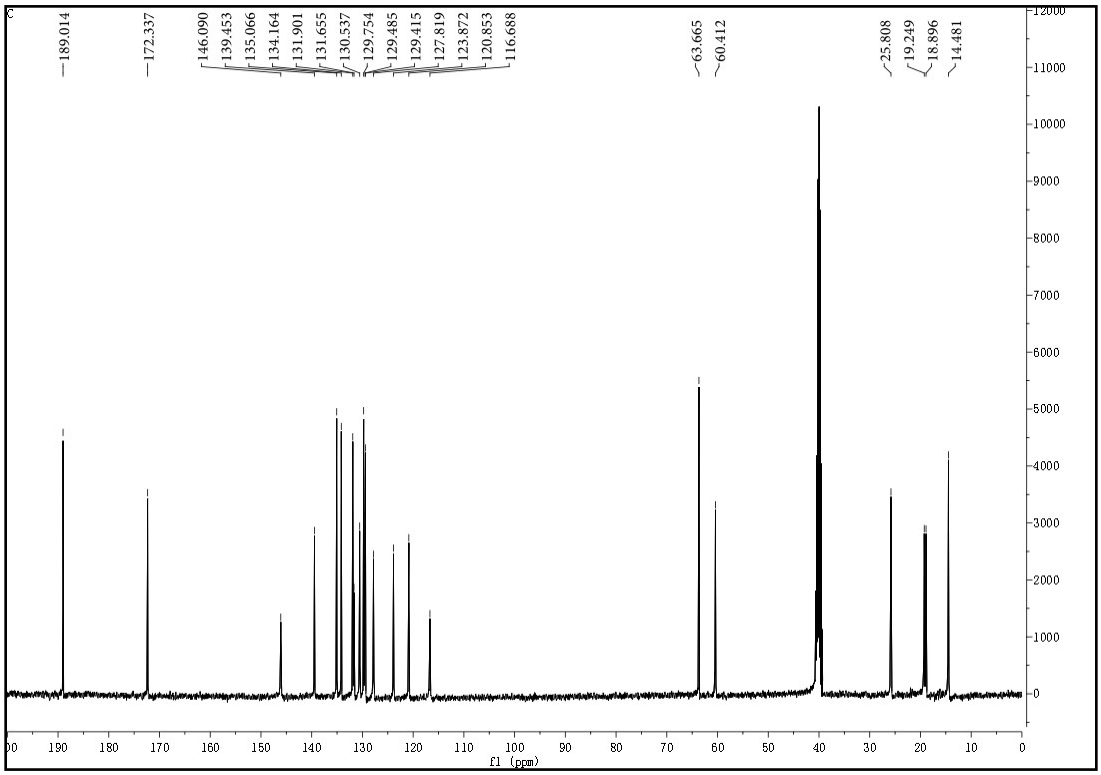

^{13}C NMR spectra of compound **8eda**

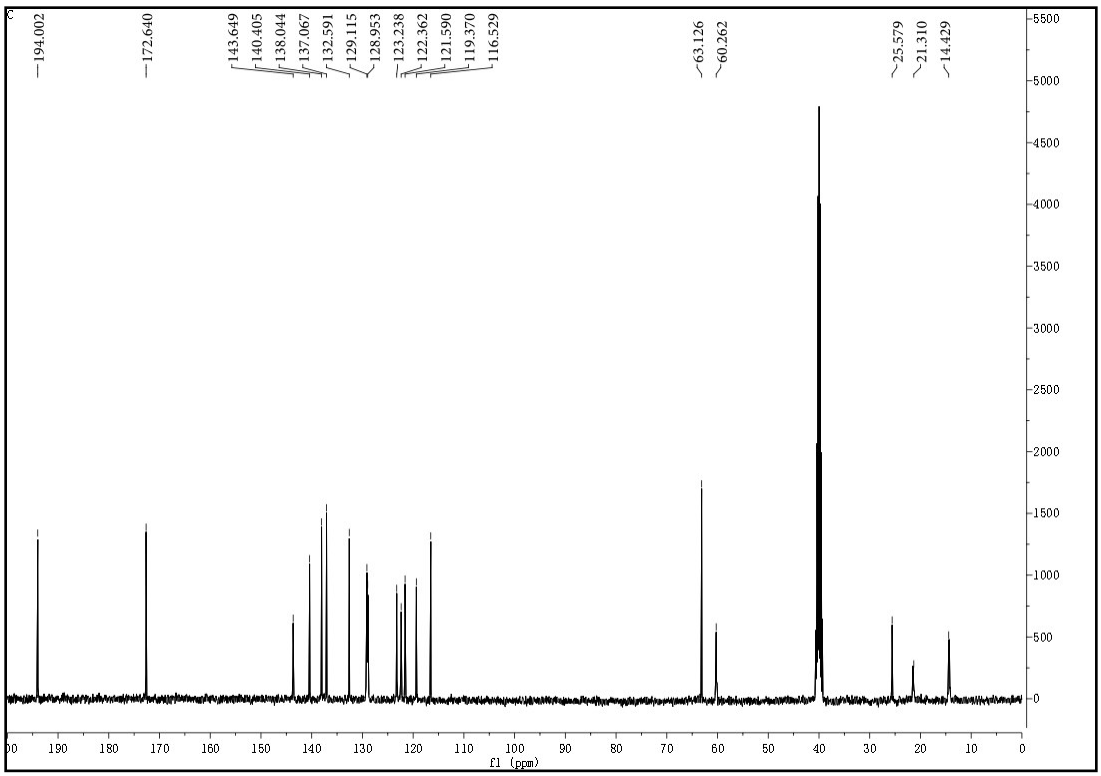

^{13}C NMR spectra of compound **8aca**

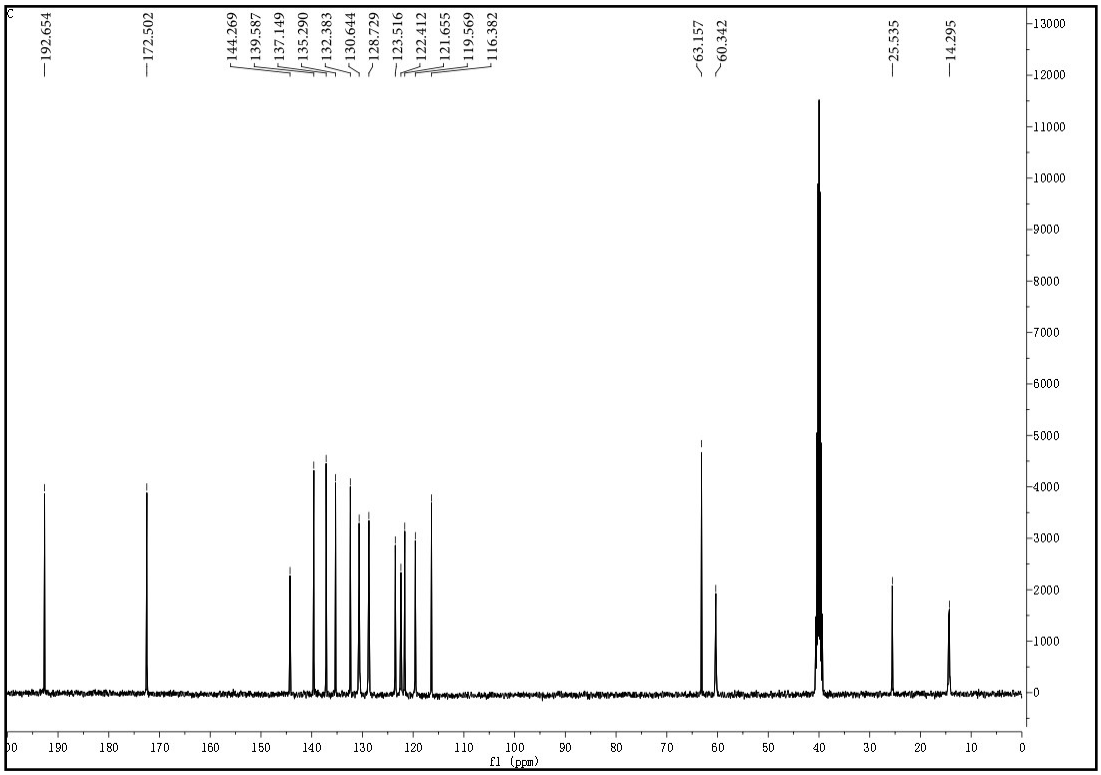

^{13}C NMR spectra of compound **8aba**

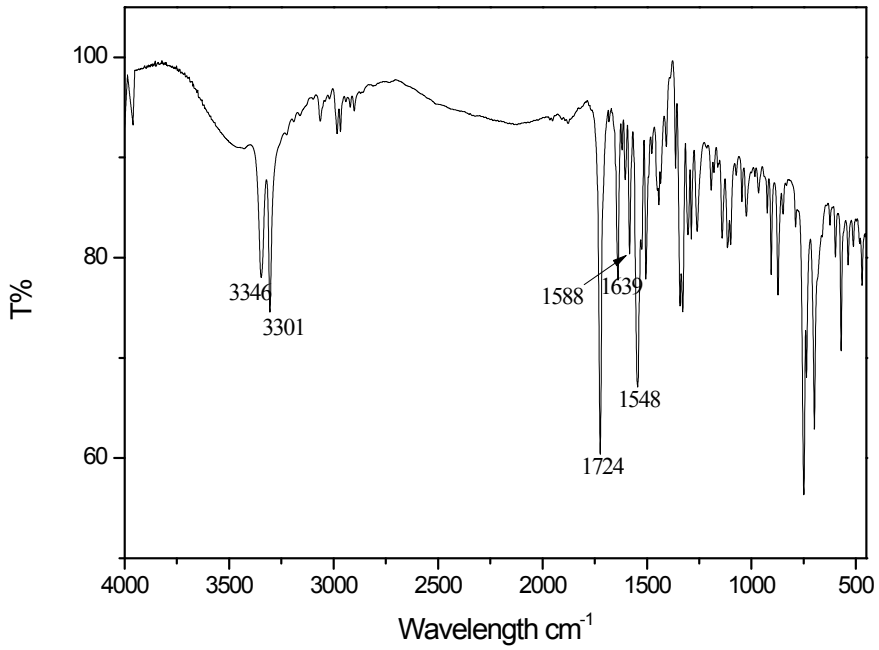
100
80
60
T%
3346
3301
1588
1639
1548
1724
4000
3500
3000
2500
2000
1500
1000
500
Wavelength cm-1

IR-**8aaa**

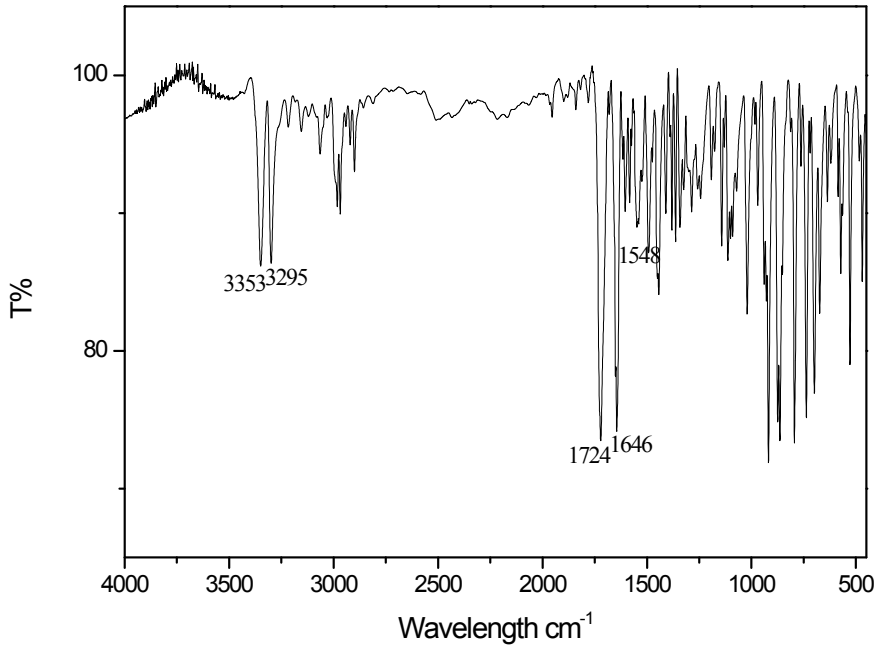
100
80
T%
3353
3295
1548
1724
1646
4000
3500
3000
2500
2000
1500
1000
500
Wavelength cm-1

IR-**8baa**

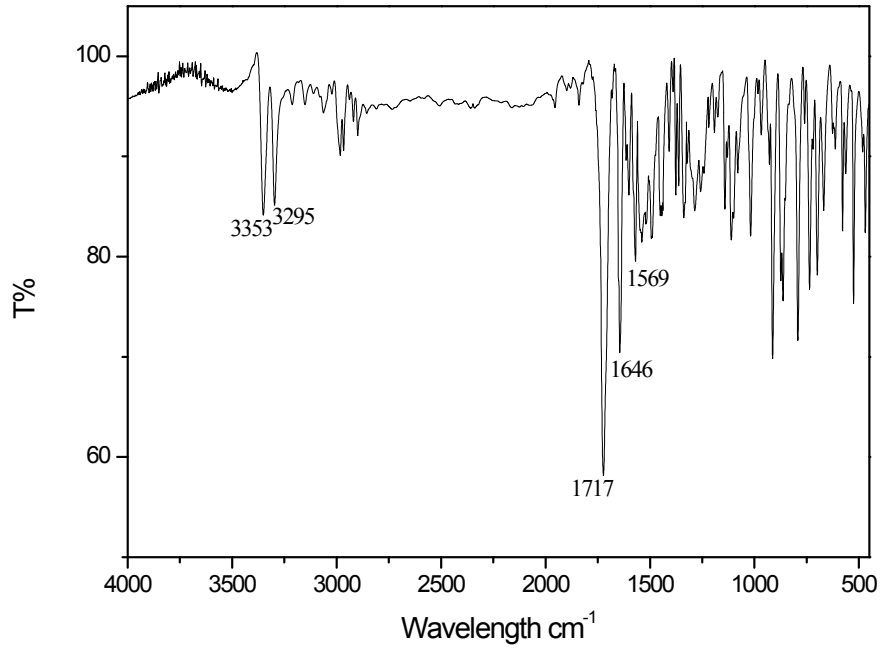

IR-**8caa**

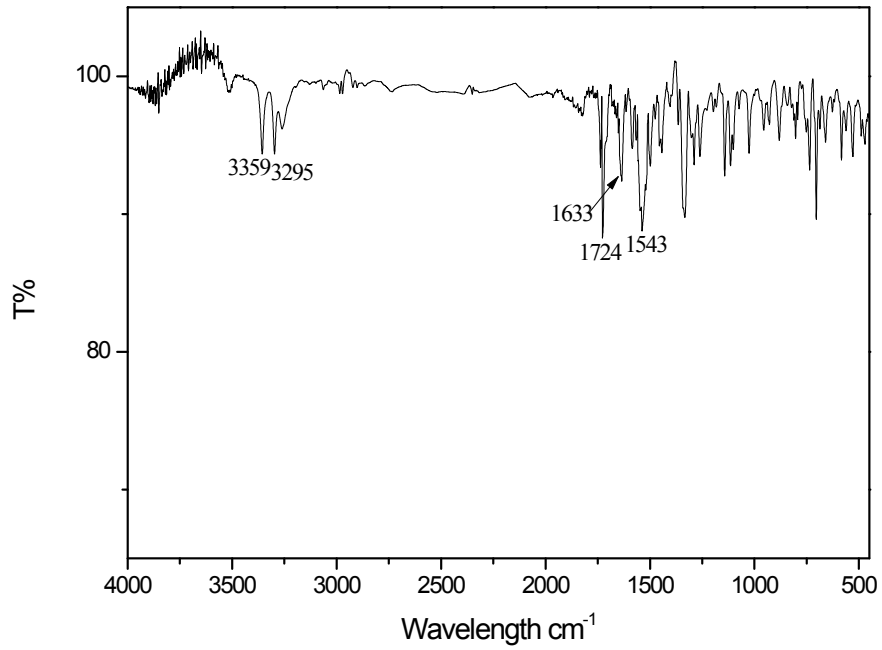

IR-**8daa**

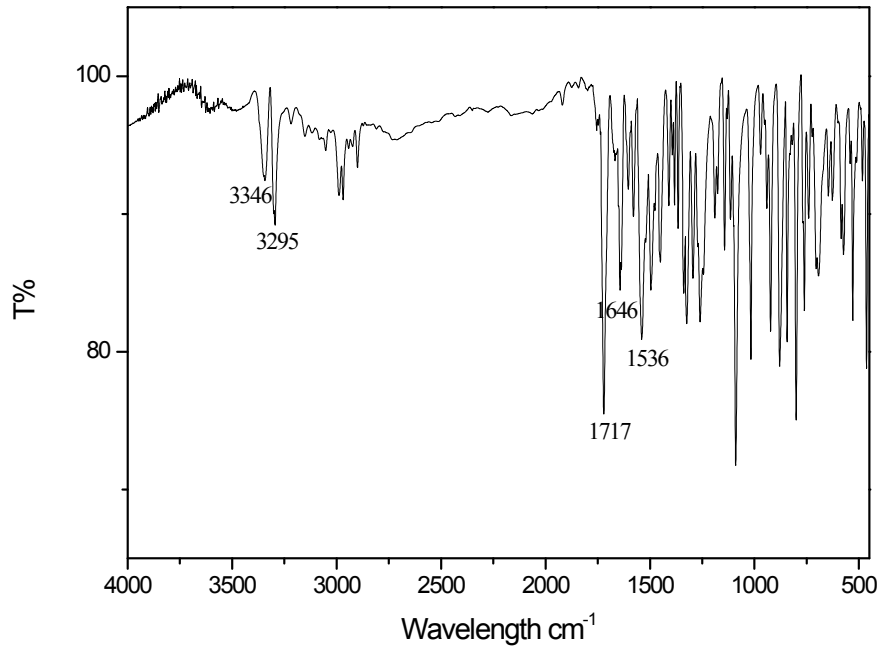
100
80
T%
3346
3295
1646
1536
1717
4000
3500
3000
2500
2000
1500
1000
500
Wavelength cm-1

IR-**8aab**

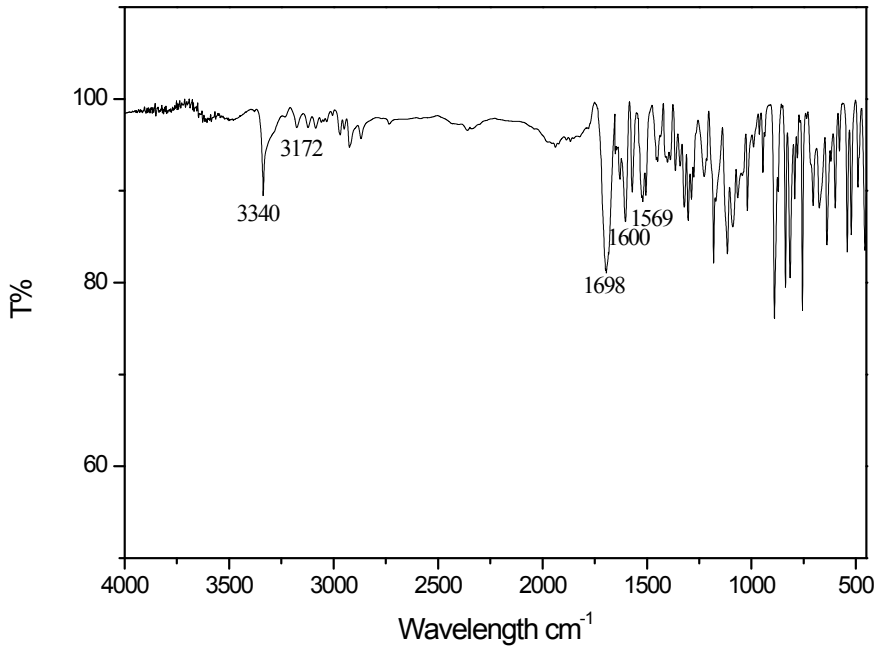

IR-**8aac**

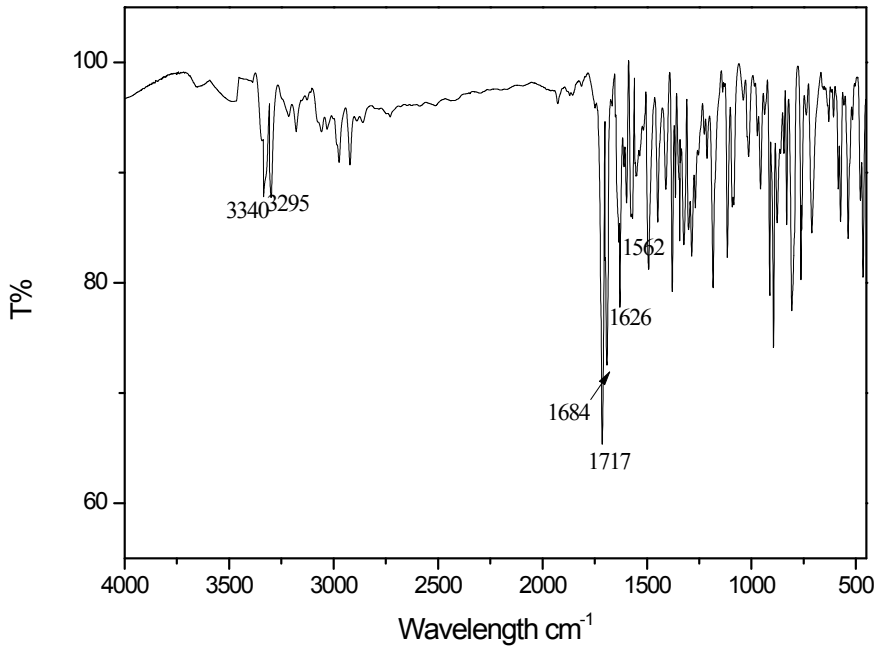

IR-**8eda**

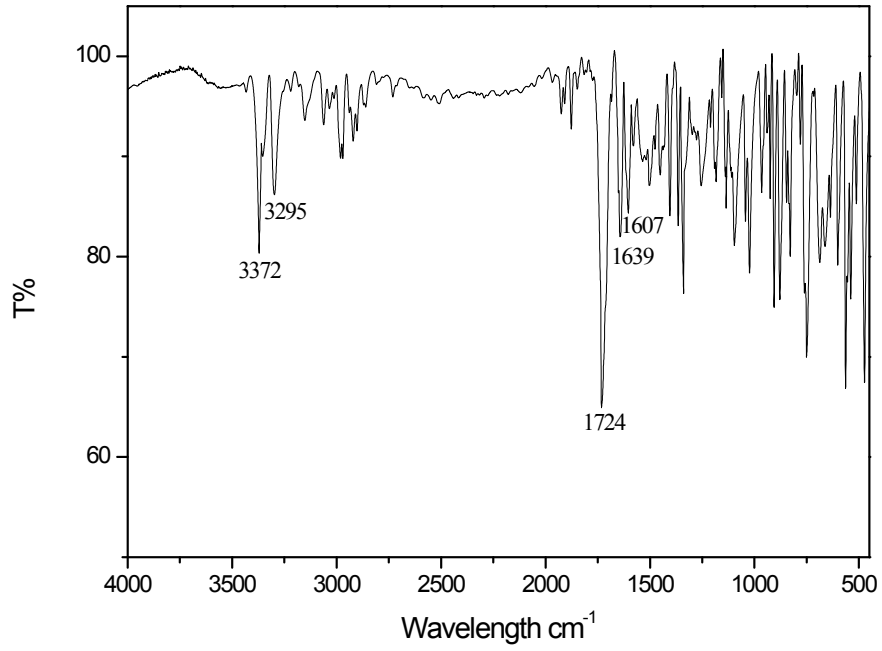

IR-**8aca**

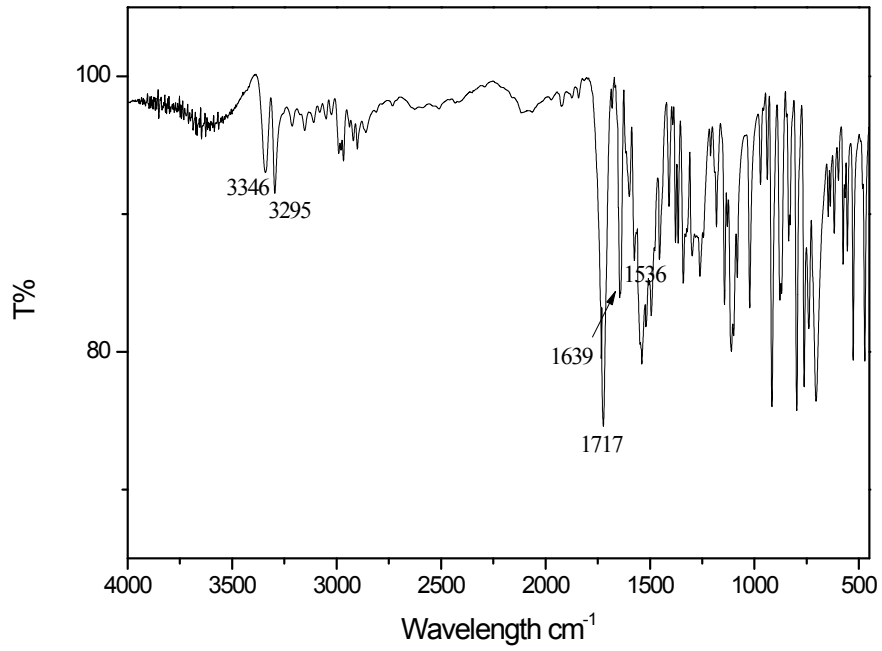

IR-**8aba**

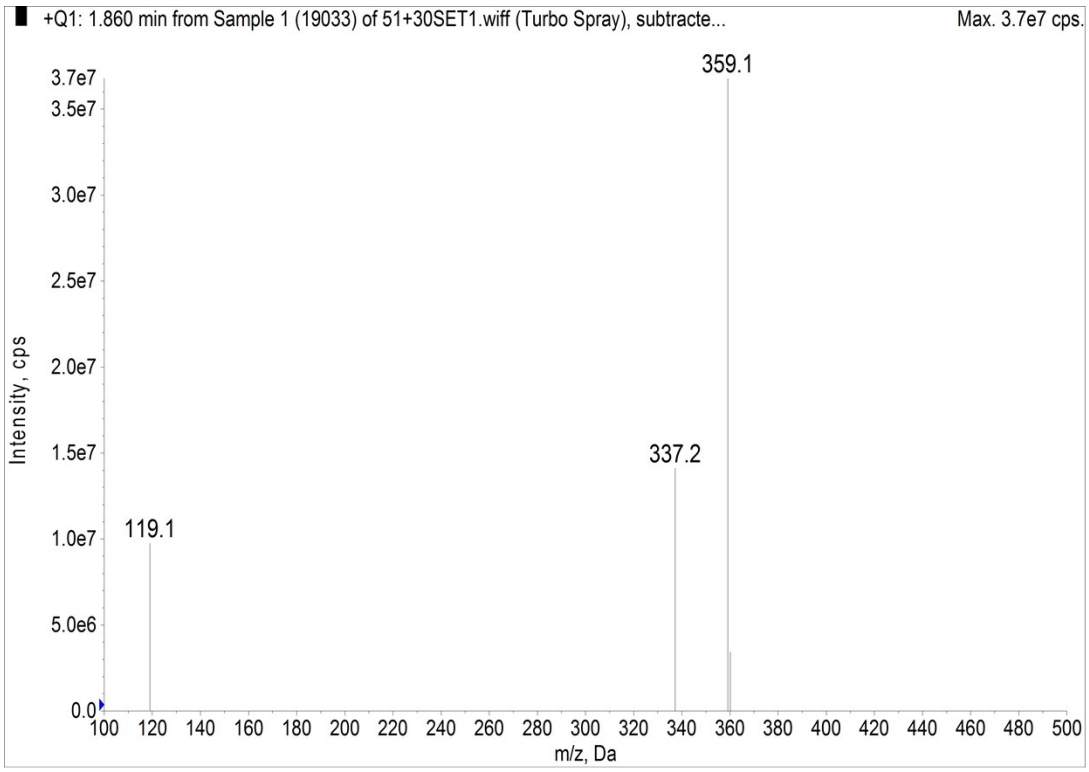

MS of compound **8aaa**

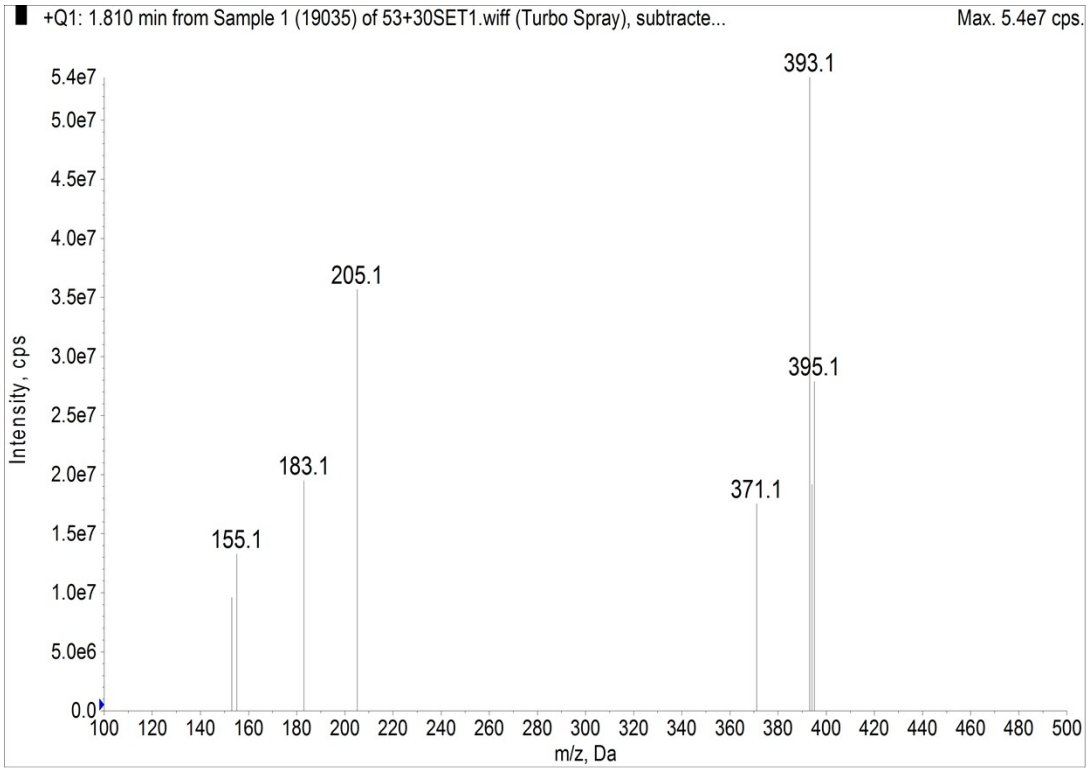

MS of compound **8baa**

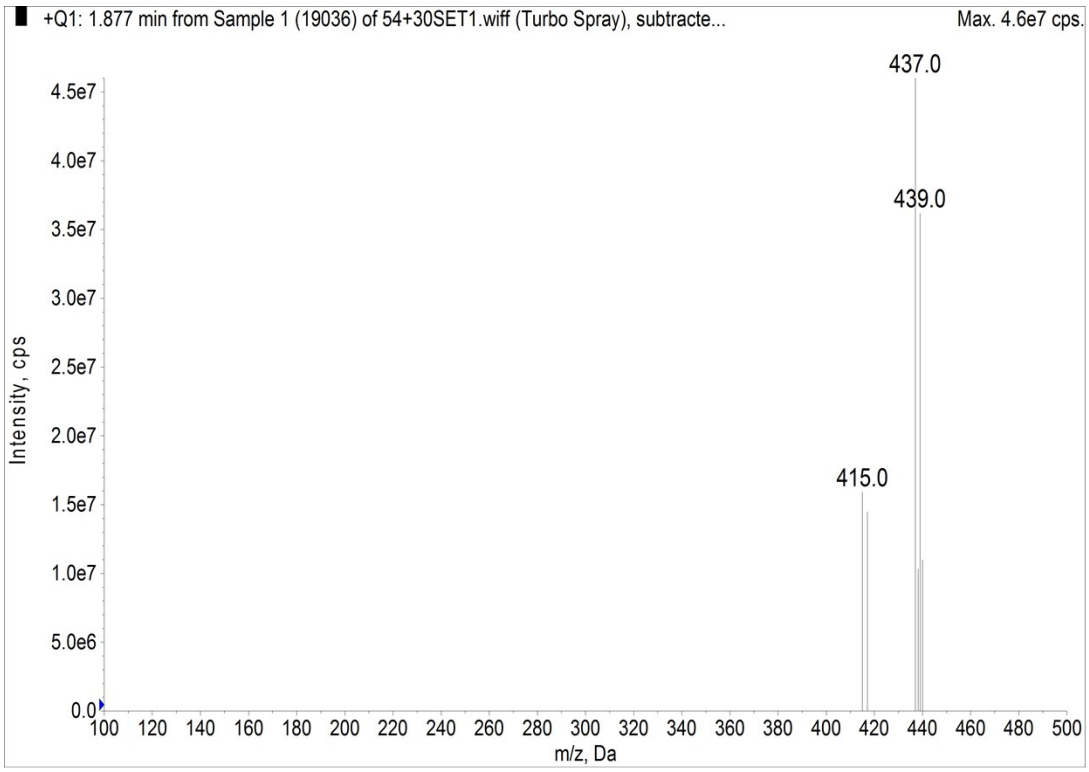

MS of compound **8caa**

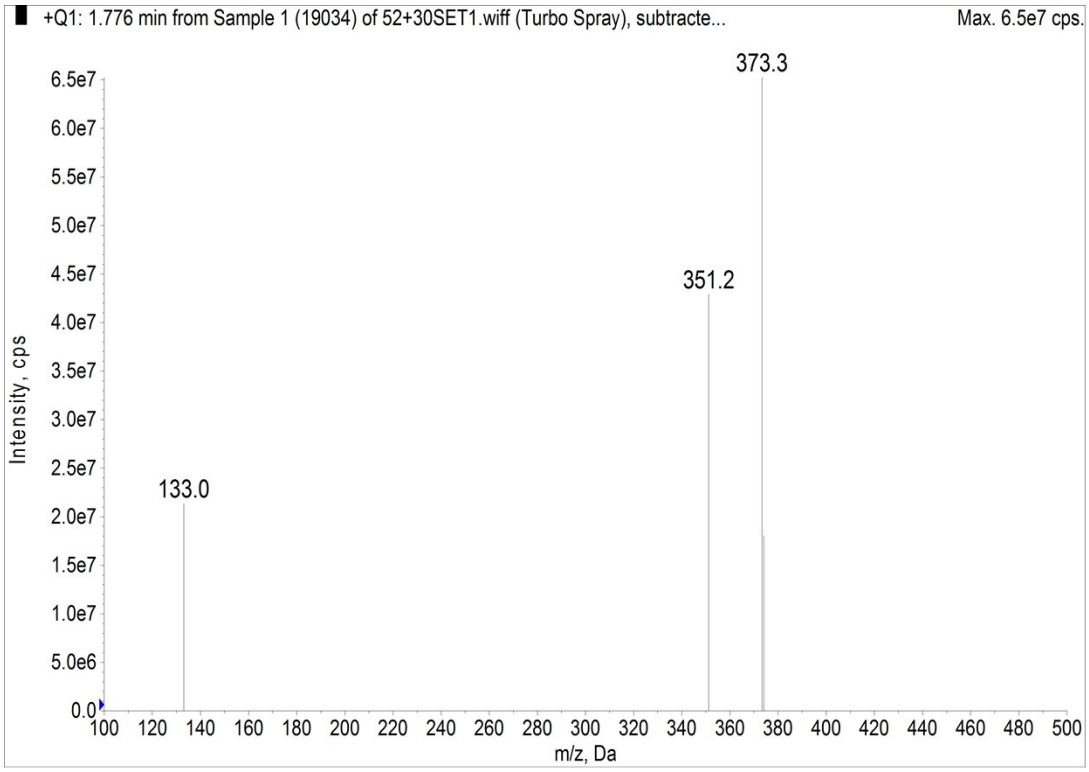

MS of compound **8daa**

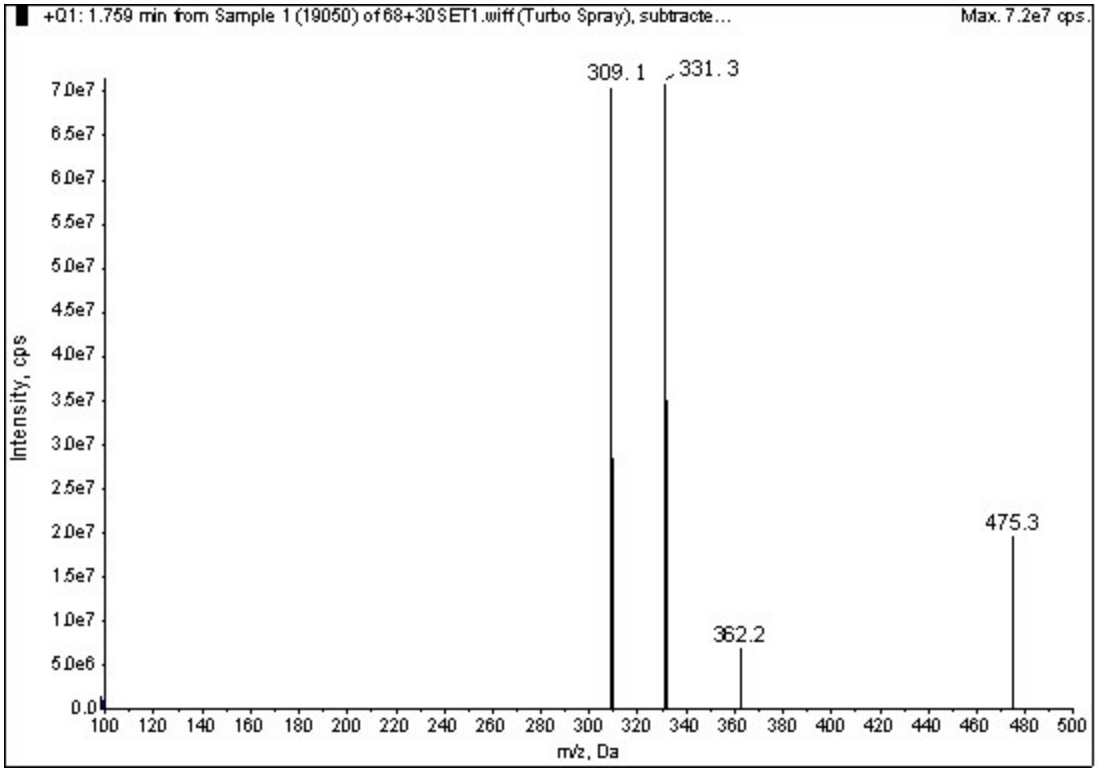

MS of compound **8aab**

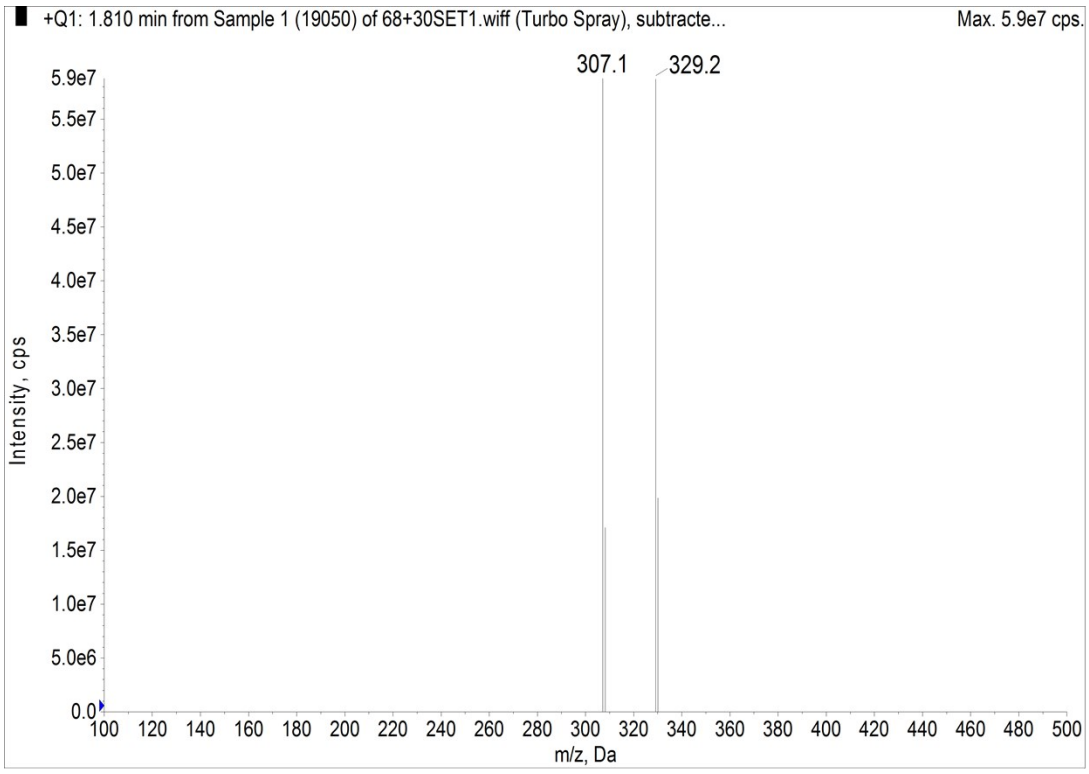

MS of compound **8aac**

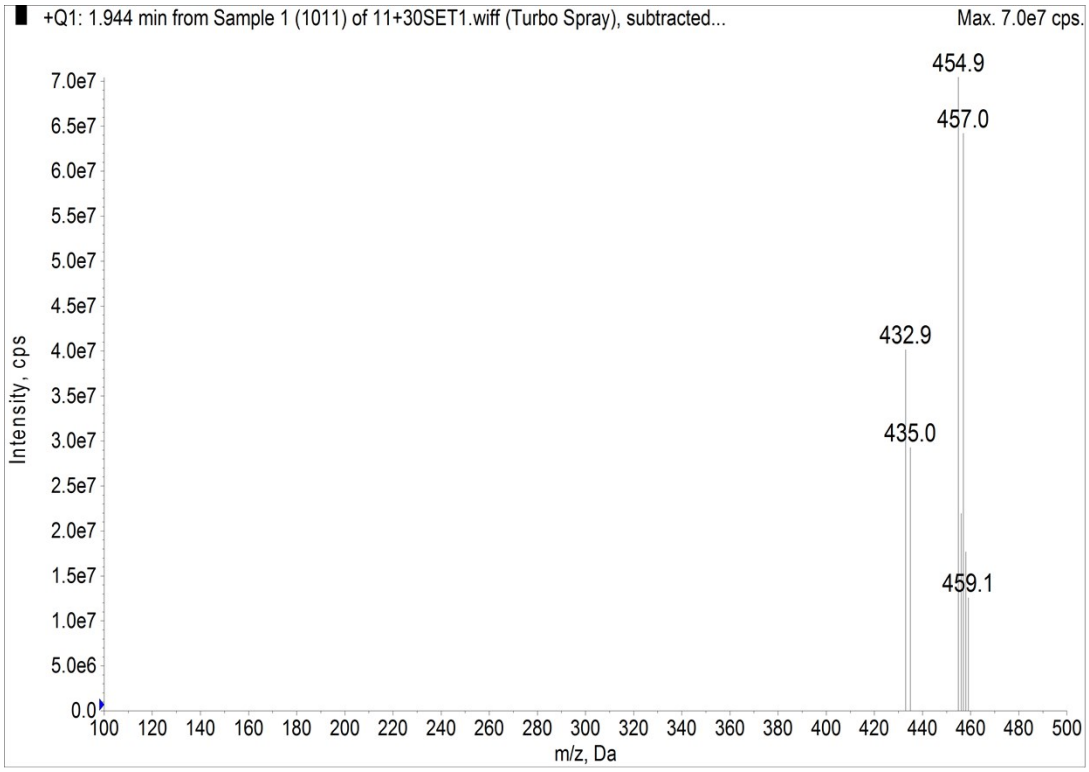

MS of compound **8eda**

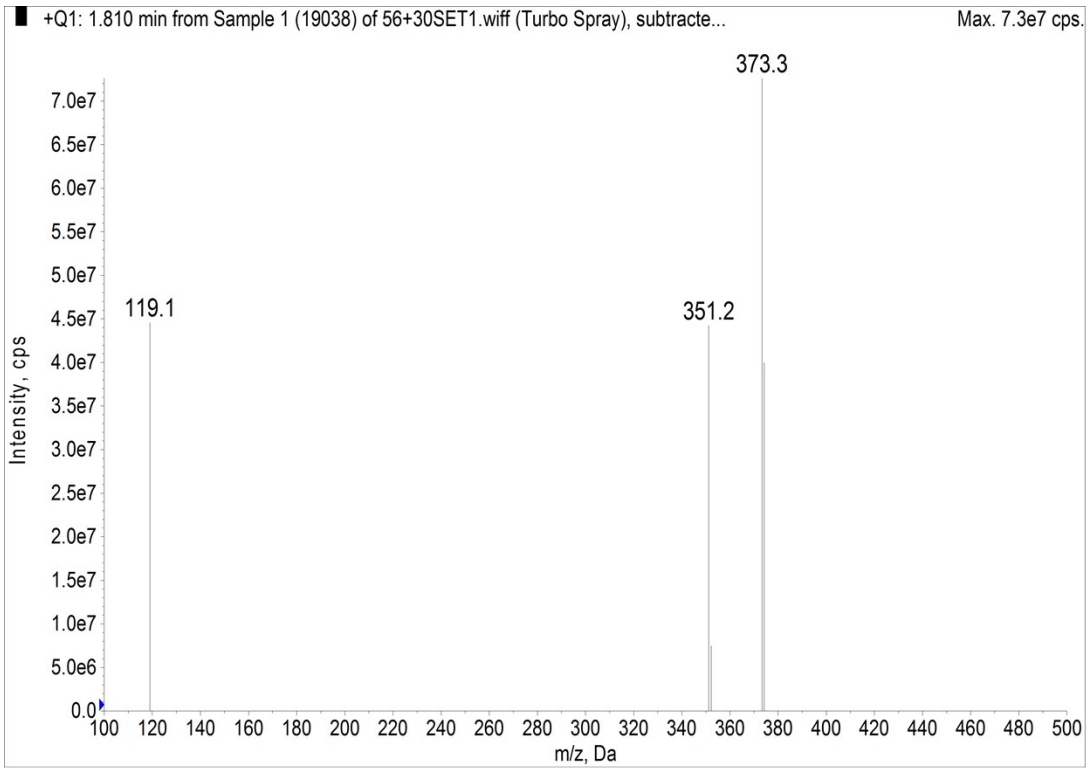

MS of compound **8aca**

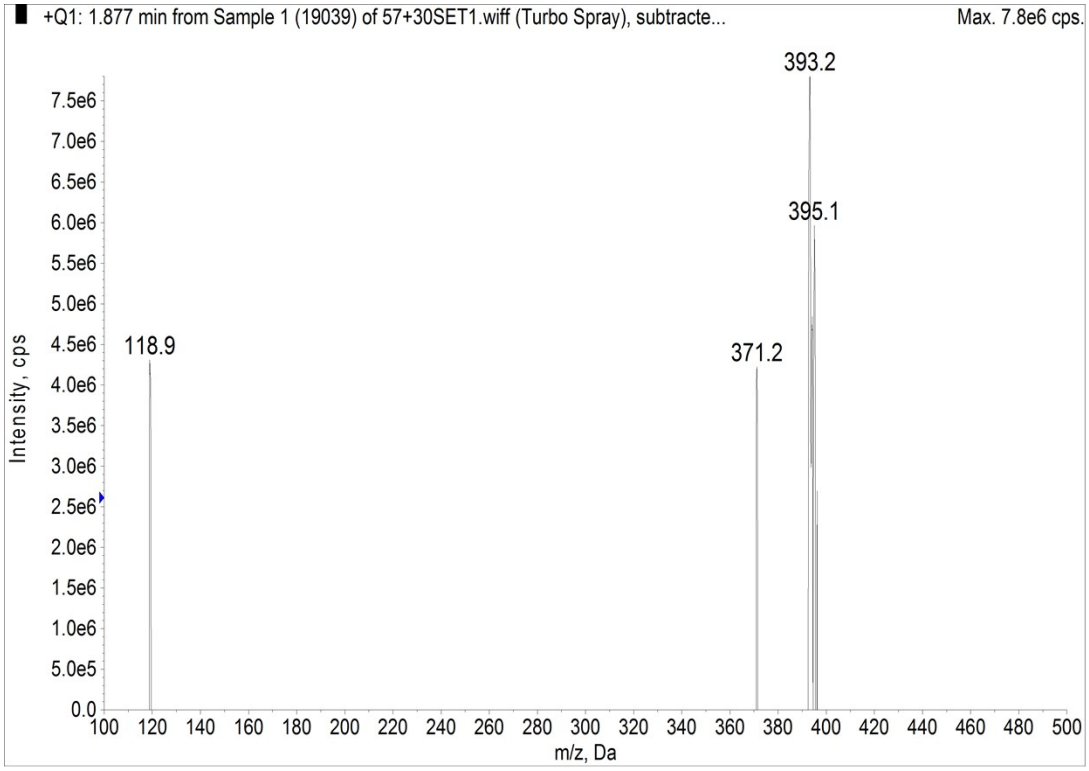

MS of compound **8aba**